NTNU
Norwegian University of Science and Technology
Department of Marine Technology

M.Sc.THESIS

Title:	Delivered:
Assessment of engine performance and exhaust emission at changing operating conditions and under fault conditions	14.06.2010
	Availability:
	Open
Student:	**Number of pages:**
Erlend Sandø Hatlevold	107

Abstract:

Performance analysis of diesel engines is an essential tool both in understanding and designing diesel engines. The analysis is also vital in predicting engine performance in different operating conditions.
In this thesis theory regarding engine performance analysis methods has been reviewed with special focus on dynamic engine process analysis. Theory on NO_x emissions has also been reviewed with special focus on thermal NO_x, since this is the main contributor to the total NO_x emission.

Engine performance for ambient and four fault conditions has been predicted for the Bergen Diesel (Rolls Royce) KRG-6 engine has been predicted by utilizing dynamic process simulation. A model of the engine has been used and calibrated in the simulation program GT-POWER. Key point parameters are presented and discussed. In addition trends for NO_x emissions are presented. The results show the importance of good maintenance and monitoring in relations to good engine performance during the engines life time.
A specific case regarding turbo charger condition for the KGJS managed MS Siskin Arrow bulk ship has been analysed by utilizing Fuel-Air process analysis. The analysis concludes with an increase of specific fuel consumption of 1 g/kWh for each 0,1 bar the charge pressure is reduced. Based on this and accurate measurements for the condition for the engine, increased cost related to fuel consumption can be estimated. Such analysis makes a good decision foundation whether and when the TC should be overhauled.

Keyword:	Advisor:
Propulsion diesel engine, performance analysis, ambient condition, fault condition, NOx	Harald Valland

Address: Location   Tel.   +47 73 595501
NTNU   Marinteknisk Senter   Fax   +47 73 595697
Department of Marine Technology   O. Nielsens vei 10
N-7491 Trondheim

NTNU
The Norwegian University of Science and
Technology

Faculty of Engineering Science
and Technology
Department of Marine Technology

MASTER THESIS

for
Stud.techn. Erlend Hatlevold
Spring semester 2010

Assessment of engine performance and exhaust emissions at changing operating conditions and under fault conditions

Vurdering av motorytelse og eksosutslipp ved endrede driftsbetingelser og ved feiltilstander.

Background

Even small reductions in fuel consumption may give significant cost savings in ship operation. Reduction in fuel consumption may in addition contribute to reduction of exhaust emissions.

Fuel consumption and exhaust emissions are affected by operating conditions of the engine and adjustments and technical capacity of various engine subsystems. Advanced control systems may allow adjustments for optimizing the performance. It is of special interest to make assessment of improvements that may be obtained by such adjustments. This assignment will focus on application of theoretical cycle computations for assessment of engine performance and exhaust emissions at changing operating conditions and under fault conditions.

Overall Aim and Focus

The overall objective of the task is to get quantitative evaluation of performance improvements that can be obtained by engine adjustments at varying operating conditions. The task should also evaluate the effect of certain fault conditions on engine performance.

The assignment should be prepared based on following points:

- Discuss the suitability of performance models with different complexity for analysis of engine performance: Seiliger process/Air-fuel process/Dynamic engine performance simulation. Make an assessment of stronger and weaker sides of the methods with regards to flexibility, accuracy and required effort to implement or make use of the methods.
- Discuss typical operating conditions for a ship propulsion engine, including variation of ambient conditions. Identify operating conditions that lead to reduced thermal efficiency.
- By means of engine performance computation, investigate how adjustments of engine parameters may improve performance at those operating conditions, and quantify the improvements.
- Identify common diesel engine fault types due to degradation during operation and describe them with respect to cause, seriousness and consequences in general.

1

- Discuss how engine faults may be introduced in performance analysis.
- Analyse a special case where a turbocharger fault gives reduced charge air pressure. Show the effect of this fault on engine performance for a two-stroke diesel engine
- Describe the method of NO_x computation in connection with engine performance analysis.

No later than 14 days after receiving the assignment the candidate should present a detailed plan for his MSc project to be approved by his teacher.

The assignment text must be included as a part of the MSc report.

The report should be written like a research report, with an abstract, conclusions, contents list, reference list, etc. During preparation of the report it is important that the candidate emphasizes easily understood and well written text. For ease of reading the report should contain adequate references at appropriate places to related text, tables and figures. On evaluation, a lot of weight is put on thorough preparation of results, their clear presentation in the form of tables and/or graphs, and on comprehensive discussion.
All used sources must be completely documented. For textbooks and periodicals, author, title, year, page number and eventually figure number must be specified.

It is assumed that the student should take initiative for establishing satisfactory contact with his teacher and eventual advisors.

In accordance with current regulations NTNU reserves the right to use any results from the project work in connection with teaching, research, publication, or other activities.

Two -2- copies of the report are required. A complete copy of all material on digital form on CD-ROM in Word-format or other relevant format should be handed in together with the written material.

The project report must be delivered no later than June 14 2010.

Department of Marine Technology, 2010-02-24

Harald Valland
professor

Preface

This report represents the work performed during my master thesis in the spring semester 2010.

 The work has consisted of several topics regarding engine performance. Understanding and preparations to use the GT-POWER simulation program has been a considerable part of the thesis. In this process the help from PhD Nabil Al Ryati has been very useful.

Further the work has been a case study regarding a specific fault condition, reduced turbocharger condition, for the KGJS MS Siskin Arrow. This case was initiated by Harald Haugen which has been most helpful in supplying needed data to perform this task.

Theory on the topics has also been a considerable part of the thesis. I have during the work gained deep understanding on the subject and been able to provide qualitative results from the simulations. Professor Harald Valland has been a great support as advisor during the period for all parts of the thesis, and for that I owe him great thanks!

Erlend Sandø Hatlevold   14.06.2010

Summary

Optimal engine performance during an engines operation lifetime is important to gain minimal costs related to fuel and maintenance cost. Downtime related to propulsion engine will also benefit from this. In this report operating conditions including ambient conditions, added loads and fault conditions for a ships propulsion engine has been identified and discussed. The main focus is on ambient conditions and fault conditions. The fault condition analysis is limited to four different conditions. Different performance models with different complexity are discussed regarding complexity, required inputs and accuracy. Dynamic process analyses are the most complex methods to use but will provide the most accurate results.

Exhaust emission theory with focus on NO_x emissions has been elaborated. It is obvious that NO_x production formed under high temperature and pressure, commonly known as thermal NO_x , is the domination contributor to the total NO_x emission from a diesel engine.

Performance analysis can involve all from single components to the entire engine. An engine model should be kept as "small" as possible but still be able to provide the desired results, this because a detailed model incorporating all engine components will require much time and processor power to calculate.

Simulations for ambient and fault conditions has been performed by utilising the computer program GT-POWER. This program is based on dynamic process analysis. A Bergen Diesel KRG-6 engine has been modelled in GT-power by the manufacturer and further calibrated during this thesis. The accuracy is within 2%. After calibration and initial simulation for standard condition, different ambient conditions has been introduced and simulated. In the table below the impact on SFC for the different ambient conditions can be seen.

Ambient air	K	275	285	295	305	315
BSFC	g/KWh	195,8	196,7	197,5	198,4	199,3
Ambient sea	K	275	285	295	305	
BSFC	g/KWh	195,9	196,7	197,4	198,2	
Humidity	%	30	40	50	60	70
BSFC	g/KWh	197,5	197,5	197,6	197,6	197,6
Ambient pressure	bar	1,022	0,972	0,922	0,872	0,822
SFC	g/KWh	197,5	197,9	198,2	198,6	199,0

Ambient conditions effect on the engine performance can be estimated by utilising calculation routines based on ISO 3046.A comparison has been made between simulations in GT-POWER and ISO corrected performance. The result deviates but shows the same trends in performance.

Four fault conditions has been introduced to the GT-POWER model and simulated with different degree of fault condition. The results show the impact of the fault condition including altered NO_x emission. Results from these simulations regarding impact on SFC can be seen in the table below.

Ambient conditions are the same for all simulations. (The blue numbers mark the initial condition for injection timing)

Compr.eff. reduction	%	100	95	90	85	80			
BSFC	g/KWh	197,5	198,8	200,2	201,8	203,6			
Turbine eff. reduction	%	100	95	90	85	80			
BSFC	g/KWh	197,5	198,8	200,2	201,7	203,4			
Inj. start rel. To TDC	deg	-8,50	-9,50	-10,50	-11,50	-12,50	-13,50	-13,50	-14,50	-15,50
BSFC	g/KWh	201,1	200,1	199,1	198,3	197,5	196,9	196,3	195,9	195,6
Cooler eff. reduction	%	100	90	80	70	60			
BSFC	g/KWh	197,5	198,1	198,7	199,2	199,8			

The fault conditions simulated will result in considerable increase of fuel consumption. This shows that proper monitoring and maintenance is beneficial. Engines operating with significant faults may not be able to produce the stated power because of parameters such as temperature and pressures are exceeding allowed limits.

A specific case regarding MS Siskin Arrow, managed by KGJS has been analysed. The propulsion engine is currently running with reduced turbocharger efficiency. The impact of this fault condition has been analysed by utilizing a Fuel-Air process model. The results from this simulation correlate with figures stated by MAN B&W regarding increase of fuel consumption for such a fault condition, which indicates an increase of 1g/kWh per 0,1 bar decrease in charge air.

Charge air pressure	Bar	1,93	1,83	1,73	1,63	1,53
SFC indicated	g/kWh	170,8	172,2	172,90	174,30	175,70
SFC effective	g/kWh	183,66	185,16	185,91	187,42	188,92

When the ship operated with a 0,2 bar reduction in charge air pressure the extra cost related to fuel will be approximately 27600US dollar per year when assumption of 200 days of continuous sailing is made.

Table of content

Figures

Tables

Abbreviations and symbols

BDC	Bottom dead centre	
CCAI	Calculated Carbon Aromaticity Index	
CR	Compression ratio	
EGR	Exhaust gas recycle	
ISO	International Organization for Standardization	
KPI	Key performance indicator	
KRG	K-type, In-line, Generator	
SMCR/MCR	Shaft Max continues rating	
TC	Turbo charger	
TDC	Top dead centre	
BSFC/SFC	Brake Specific fuel consumption	g/kWh
IMEP	Indicated mean effective pressure	bar
LHV	Lower heating value	KJ/KG
MEP	Mean effective pressure	bar
ROHR	Rate of heat release	$\dfrac{dQ}{d\varphi}$
a	Iso-volumetric ratio	-
a	Humidity factor	-
b	Isobar ratio	-
c	Isotherm ratio	-
f	fuel-air mass ratio	-
F	Fuel-air equivalence factor	-
h	Specific enthalpy	KJ/kg
k	Ratio of indicated power	-
m	Mass	kg
m	Exponent ; dry air pressure ratio or total barometric pressure ratio	-
n	Exponent; ambient air thermodynamic temperature ratio	-
p	Pressure	bar
Q	Heat	kJ
R	Gas constant	KJ/kgK
s	Specific entropy	KJ/kg
s	Exponent; charge air coolant thermodynamic ratio	-
T	Time	Sek
T	Temperature	K or C
u	Internal energy per unit mass	KJ/kg
V	Volume	m^3
w	Specific work	kJ/kg
W	Work	kJ

C_p	Specific heat at constant pressure	kJ/kg*K
C_v	Specific heat at constant volume	kJ/kg*K
f_s	fuel-air mass ratio, stochiometric	-
h_L	Lower heating value	kJ/kg
k_i^+, k_i^-	Reaction speed constant	-
m_a	Mass; air	Kg
m_f	Mass; fuel	Kg
$\dot{m}$	Mass flow	Kg/s
n_c	Polytrophic compression exponent	-
P_{comp}	Pressure after compression	bar
P_{H_2O}	Partial pressure for water vapour in the gas	bar
$P_{H_2O}^*$	Water vapour saturation point for the gas temperature	bar
$P_{mi} = IMEP$	Indicated mean effective pressure	Bar
p_{ra}	Substitute reference total barometric pressure	kPa
P_x	Power for site ambient condition	kW
P_0	Ambient pressure	bar
$\dot{Q}$	Heat flow	kJ/s = kW
Q_c	Heat from combustion	kJ
Q_{HT}	Heat loss due to heat transfer	kJ
r_c	Compression ratio	-
r_r	Boost pressure ratio under standard reference conditions	
T_{cra}	Substitute reference charge air coolant thermodynamic temperature	
T_{ra}	Substitute reference ambient air thermodynamic temperature	K
V_{TDC}	Volume at top dead centre	m^3
V_{BDC}	Volume at bottom dead centre	m^3
V_C	Compression volume (inlet and exhaust valves closed)	m^3
$\emptyset_r$	Relative humidity for air	%
α	Power adjustment factor	-
β	Specific fuel consumption adjustment factor	-
ε	Geometric compression ratio	-
κ	Gas constant	-
η	Efficiency	-
π_1	Pressure ratio; ambient – charge air	-
φ	Crank angle	º

1. Introduction

Fuel costs and environmental footprint is becoming more and more important today for all kind of transportation. Sea transport is known to be the most environmental way to perform transportation. The diesel engine is the most common prime mover used for ship propulsion today as it has been for the last 30 years. The reason for this is the superior efficiency compared to other thermal engines. However the propulsion engine for large ships consumes large quantities of fuel during a year and represents a large percentage of the total operating cost. Alterations in a ship propulsion engines operating condition will rapidly lead to increased fuel consumption, which will give a significant increase in fuel cost. The modern diesel engine is a very complicated system due to the turbo charger and other subsystems. Its performance is monitored by measurable engine parameters such as exhaust temperature and cylinder pressure diagrams. Even with these data collected, it is extremely difficult in many cases to determine the cause of reduced performance due to a fault condition, due to the complexity of the engine. To identify the different fault conditions from another, engine simulation can provide important information both on fault conditions and operating conditions. Different types of simulation models regarding complexity such as simple cycle analysis (Seiliger or fuel/air) or dynamic processes are available. These will be discussed in the beginning of the report with focus on complexity and accuracy. During this thesis impacts from ambient conditions will be investigated by means of an advanced simulation program called, GT-POWER. The work in this thesis regarding fault conditions will be limited to four typical fault conditions. These will also be simulated in GT-POWER. A specific case regarding reduced turbine condition will also be analysed with focus on the increase in fuel consumption. This will be done by means of a Fuel-Air analysis model.

2. Suitability of performance analysis models

There are several engine performance analysis models with different level of complexity available to predict the engine's performance. Simple models require less data and less computation, but will not provide as accurate results. Usually the "in cylinder" process is in focus when performing traditional performance analysis. Components such as the turbocharger, charge air cooler, air filter and gas flow in the different pipes can be modelled and incorporated in a complete model. This is done in the simulation model for the Bergen diesel KRG engine in chapter 8. Separate models for these components can easily be set up based on isentropic or polytrophic processes for the turbine and standard heat changer theory. One-dimensional flow in pipes is often used to model pressure drop in pipes. In this chapter, three widely used models for "in cylinder" processes will be described and discussed, focusing on complexity, accuracy and when the models are applicable.

2.1. Seiliger process/air process

The development of simple performance analysis began soon after the first successful diesel engine trial in 1895. The accuracy of the calculations was not good, but gave a good picture of the expected performance of a diesel engine. In 1922 M. Seiliger introduced an improved method to compute performance in cylinder processes. The method enabled analysts to shape the process in the cylinder in a more realistic way. This was done by introducing the "6-point" cycle. To shape the process he introduced shaping parameters (a, b, c) so that the iso-volumetric combustion, isobaric combustion/expansion and isothermal combustion/expansion could be expressed. The Seiliger cycle could be used for both Diesel and Otto processes (Stapersma 2009).

The method

The stages in one cycle in a diesel engine can be broken down into separate processes as shown in figure 1. These processes are intake, compression, combustion or heat input, expansion and exhaust. In addition the processes in the air supply and exhaust system can be modelled and analysed. These are not included in this performance analysis but will give input data to the combustion such as pressure and temperature for the air going into the process analysis of the combustion. In an air cycle analysis several assumptions and simplifications have to be done. These are:

Assumptions of

- constant C_p and C_v values during the different processes (may be estimated for each stage)
- Constant mass
- End state calculations for the different processes.
- Expansion ends at the same volume as compression starts (may be modified)
- No heat loss during expansion and compression

Today these types of models are useful to get an overview of the processes carried out in a diesel engine typically in an early design process or for educational purposes. The air cycle analysis will not give qualitatively results for a real engine cycle (Heywood 1988).
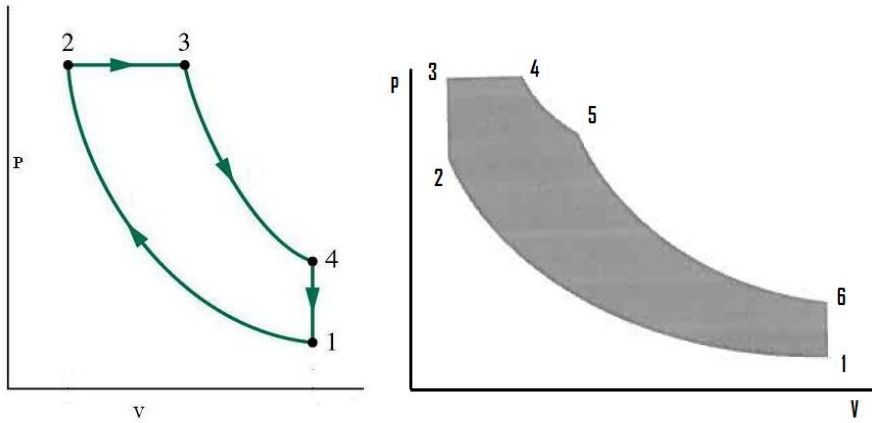
Figure 1 Ideal Diesel process and Seiliger cycle (a, b, c differs from 1)

Figure 1 shows to the left a typical ideal diesel process and to the right a 6 stage Seiliger cycle. The three stages 2-3, 3-4 and 4-5 in the Seiliger process are adjusted by altering the parameters:

$$a = \frac{P_3}{P_2} \qquad (2.1)$$

$$b = \frac{V_4}{V_3} \qquad (2.2)$$

$$c = \frac{T_5}{T_4} \qquad (2.3)$$

If the Seiliger cycle should represent an ideal Diesel process, then c=a=1 (Hatlevold 2009)The fifth point representing isothermal expansion/combustion is often excluded when analysing the diesel process.

The theoretical efficiency can be determined by the following equation:

$$\eta_{th} = 1 - \frac{1}{r_c^{\gamma-1}} * \frac{a * b^\gamma * c^{\gamma-1} - 1}{\{(a-1) + \gamma * a * (b-1) + (\gamma-1) * a * b * \ln(c)\}}$$

(2.4)

The theoretical specific fuel consumption can then be determined by:

$$sfc_{th} = \frac{3600000}{\eta_{th} * h_L}$$

(2.5)

The theoretical IMEP for the Seiliger process can be determined from the following expression:

$$P_{mi,th} = P_0 * \pi_1 * \frac{r_c}{\varepsilon - 1} * \eta_{th}$$

$$* \frac{r_c^{\gamma-1} * \{(a-1) + \gamma * a * (b-1) + (\gamma-1) * a * b * \ln(c)\}}{\gamma - 1}$$

(2.6)

and is a function of the following parameters

$$f(p_0, \pi_1, \varepsilon, r_c, a, b, c, \gamma)$$

p_0 Ambient pressure
π_1 Trapped pressure ratio
ε Compression ratio
r_c Effective compression ratio
γ Ratio of specific heat
h_L Lower heat value

By manipulating the parameters the trade-off effects can easily be determined with this type of analysis. The mechanical dimensions of the engine are not present so far but can be determined based on desired brake power and compression ratio.(Stapersma 2009)

The Seiliger process is as discussed a simple performance analysis model with several limitations, as described earlier, and will therefore provide inaccurate results. However, since the model is simple, it is quite easy to use and will provide answers that roughly correspond to a real engine cycle. This type of model is often used for educational purposes and can give good understanding on how alterations of key parameters will affect the performance. Using this kind of model for detailed performance analysis as will be performed in this master thesis, will not be sufficient to provide the results needed.

2.2. Fuel-Air process

The air-fuel cycle is based on the air cycle analysis. Normally, five processes are used to define the cycle in a diesel engine. In addition the fuel-air equivalent factor (F) is introduced in all processes. F will, in an ideal cycle, be zero during compression as the working media is 100% air. As the combustion starts F will increase until it reaches its maximum. During scavenging and air inlet stroke, F will return to zero. As there are some residual gases left in the cylinder after scavenging, F will never be zero for a real cycle. Since there are 3 variables to be illustrated it is beneficial to illustrate it in a PVF diagram. Figure 2 shows a 3-dimensional diagram presenting a 4 stroke engine cycle process.
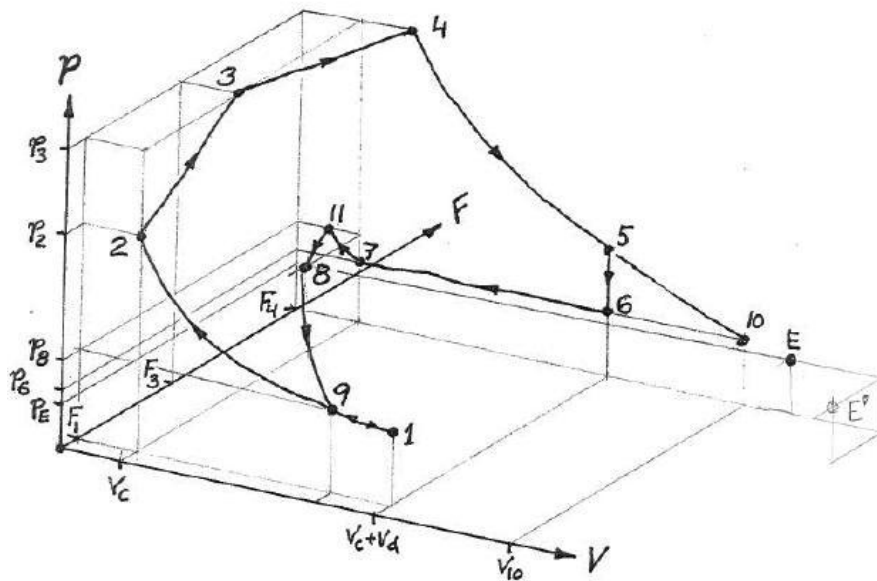
Figure 2 Air- fuel cycle presented in PVF diagram for a 4 stroke diesel engine (Valland(a))

The diagram is based on the processes from the program called "POWER CYCLE". The stages used in the diagram presentation are defined as:

1-2   Compression
2-3   Combustion constant volume
3-4   Combustion constant pressure
4-5   Expansion
5-6   Blow down
6-7   Exhaust stroke
8-9   Inlet stroke
10   Represents complete expansion to exhaust receiver pressure
7-11-8   Represents equalising of pressure during opening of
         Inlet valve and closing of exhaust valve

Table 1 Definition of stages in fuel-air cycle for a 4 stroke diesel engine

In this type of analysis the composition of the working medium is modelled and the alteration during the process is included in the analysis. This means that R (gas constant) is a function of pressure, temperature and fuel-air equivalence factor.

$$F = \frac{\frac{m_F}{m_A}}{\left(\frac{m_F}{m_A}\right)_s} = \frac{f}{f_s} \tag{2.7}$$

By including this parameter, more accurate results are achieved than with the air cycle analysis. The analyses require more calculations and are therefore usually performed by utilising computer programs.

Method

The computation is similar to the one for air cycle, but requires input for F and calculations for working media properties. The compression process is calculated in the same way as for the air cycle. The variation in n_c is small and a middle value is used. Calculation of combustion needs input for the end state (F, pressure, m_F or temperature). One of these variables has to be known to calculate the end state values. Assuming that F_2 (end state after combustion at constant volume) is known, the alteration in internal energy for combustion at constant volume can be determined by:

$$u_2 = \frac{(1 + f_s F_1) u_1 + f_s (F_2 - F_1) h_F}{1 + f_s F_2} \tag{2.8}$$

The other state variables (p, T, s, h,) can now be determined for the state.

The specific enthalpy for combustion during constant pressure can be determined similarly (F_2 end state after combustion at constant pressure):

$$h_2 = \frac{(1 + f_s F_1) h_1 + f_s (F_2 - F_1) h_F}{1 + f_s F_2} \tag{2.9}$$

Expansion is calculated in the same way as for the simple cycle, but since the gas composition is different, other gas properties are used. (Hatlevold 2009)

This kind of engine simulation is also relatively easy to perform and does not require very much engine data. The simulation will provide reasonable but not accurate results. The computation is relatively complex compared to air process simulations as more data is required and fewer assumptions have to be made. Computer aid is necessary when performing simulations and especially multiple simulations. Trends for the engine performance when one or several parameters are changed can be developed based on key data. The air fuel simulation will be used when investigating the impact on a diesel engine when charge air pressure is reduced due to decrease of turbo charger efficiency.

2.3. Dynamic processes

Dynamic process analysis is the most complex analysis that can be performed when analysing the diesel engine. The core of the analysis is the "in cylinder" process. The analysis can be performed in different complexity studying only single components as the compressor or the combustion process or it can incorporate the whole engine. The following summary of the dynamic equation analysis is retrieved from the pre project delivered autumn 2009.

2.3.1. Dynamic equation analysis

In the previous chapters, air cycle and air fuel cycle analysis has been discussed. These are classical engineering thermodynamic analysis that splits the total cycle into several processes, i.e. compression / combustion. In reality the processes require time to complete, but time is not a variable in simple cycle analysis.

The processes carried out in a diesel engine will depend on flow rates and are therefore not a classic simple process. Consequently time is an important variable when carrying out such process analysis. The processes are described as dynamic processes, because the time is brought in as a free variable.

Dynamic state equations are used to model the processes in the diesel engine. There are several approaches to how a model can be built. Dynamic equations will briefly be elaborate on the assumptions of open and closed system approach and what limitations they have.

The method can be applied to many problems. The complexity depends on what results the model should provide. (Valland(c) 2008). For this master thesis, a dynamic model will be used to predict engine performance. Manual calculations are very time consuming and complex, and will not be a part of the master thesis. The dynamic state equations are partly the background for the computer program GT-POWER which will be elaborated later.

The Method

To create a model that reflects a real diesel engine, very detailed input data is required. Sub models can be implemented to model the airflow outside the cylinder (Turbocharger, cooler, filter, silencer and ducts). The following elaboration is based on the lecture notes in the course Combustion engines, and is limited to the "in-cylinder" process. (Valland(c) 2008)

Time

When computing the process in a diesel engine, it is beneficial to use the crank angle instead of the time. This is understandable since the position of the piston directly controls the processes in a diesel engine. The relation is easily converted by the following expression:

$$\varphi = \omega * t + \varphi_0 \qquad (2.10)$$

2.3.1.1. Closed system approach

With the closed system approach it is assume that the cylinder volume is a closed system. This means that the process is studied when the volume is closed off, i.e. both valves are closed (Compression, combustion and expansion).

It is further assumed that the working medium composition is constant and ideal. The interaction with the surroundings is only done with heat exchange through the walls. By setting these restrictions, the combustion taking place can only be represented by heat addition equivalent to the combustion. The process can therefore be described inside the system with the first law of thermodynamics and the gas equation for ideal gas.(Valland(c) 2008)

First law:
$$dU = mc_v dT = dQ - pdV \qquad (2.11)$$

Gas law:
$$\frac{dp}{p} + \frac{dV}{V} = \frac{dT}{T} \qquad (2.12)$$

By combining the two equations and differentiate to crank angle we can derive an expression for net heat flow:

$$\frac{dQ}{d\varphi} = \frac{1}{\kappa - 1}\left[V\frac{dp}{d\varphi} + \kappa p\frac{dV}{d\varphi}\right] \qquad (2.13)$$

This is the heat pr. degree unit or rate of heat release ROHR. By use of volume function and pressure function, the net heat flow into the cylinder can be determined. The net heat flow can be separated into two categories; the heat of combustion and the heat transfer.

$$\frac{dQ}{d\varphi} = \frac{dQ_c}{d\varphi} - \frac{dQ_{HT}}{d\varphi} \qquad (2.14)$$

By equation 2.14, the heat flow during compression and expansion is determined directly, as the heat flow is entirely due to heat transfer out of the system. The gas composition is not the same during the two processes (compression and expansion), but are constant for both processes and must be taken into consideration.

By assuming constant gas composition during combustion, the ROHR can easily be determined and plotted. It has been shown that the pattern of this curve is approximately correct even if that assumption is made. (Valland(c) 2008)
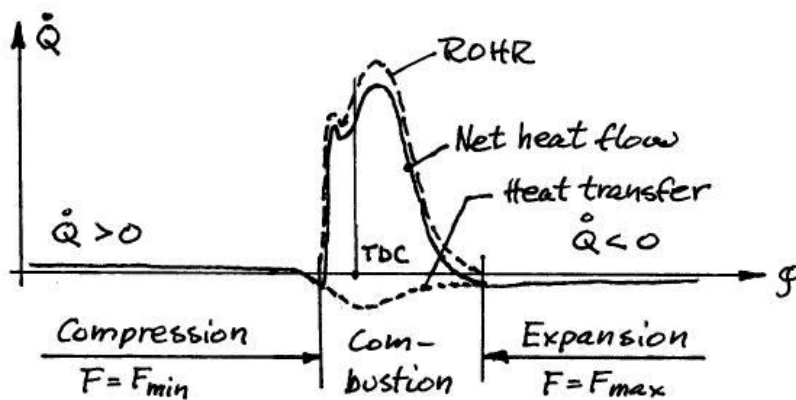
Figure 3 ROHR determined from closed system approach

The ROHR curve provides important information about the combustion. Duration of combustion, intensity of the premixed-combustion phase and total energy release during the combustion can be determined from the ROHR.

The ROHR curve is based on measured cylinder pressure. These measurements are sensitive and often difficult to get correct. Reasons for this are:

- It is difficult to define accurate point of TDC.
- Measurements of cylinder pressure are done with equipment that measure relative pressure. The actual pressure level must be corrected with a pressure difference Δp.
- The exact compression ratio ε is normally not known.

There exist methods to correct these errors. (Valland(c) 2008)

Dynamic cylinder pressure
If the heat loss and the heat of combustion are known, the pressure differential differentiated with respect to the crank angle can be determined in a similar way.

$$\frac{dp}{d\varphi} = (\kappa - 1)\frac{1}{V}\frac{dQ}{d\varphi} - \kappa\frac{p}{V}\frac{dV}{d\varphi} \tag{2.15}$$

The pressure can then be plotted.
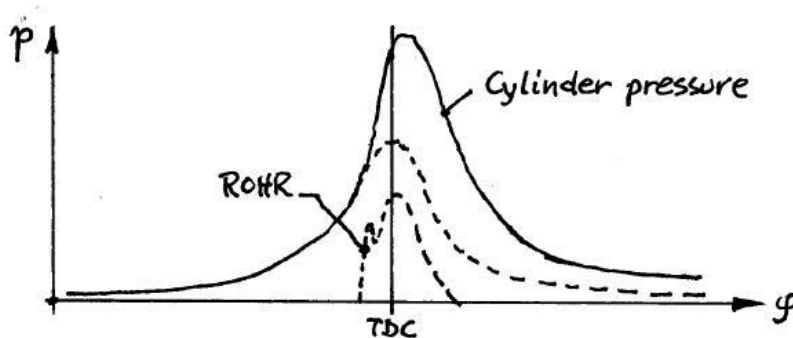
Figure 4 Dynamic cylinder pressure

The temperature can be determined by use of the gas equation.

The equations for ROHR and dynamic pressure are valid for closed systems with ideal gas with invariant composition. We can enhance the computation by letting the heat capacities be functions of temperature instead of fixed values. This is however a much more complex process.

As described above the ROHR or pressure function can be calculated, depending on which is known. The methods are relatively simple to compute and get the desired result, but have relatively large limitations. The main limitation is related to the assumption of fixed gas composition. Further the method can only compute processes when the cylinder is closed and it does not take into account gas leakage from the process that will occur (Valland(c) 2008). However the shape of the curve computed with closed system approach is similar to a "real" ROHR curve, and will therefore be a good indicator on the combustion development with limited effort in calculations.

The limitations mentioned can be lifted by looking at the process as an open system. This allows bringing the mass flow in and out of the system and taking the change in gas composition into consideration.

2.3.1.2. Open system approach

In this type of calculations mass flow and working media composition is brought in to the model. Several differential equations are required to perform the calculations. The following elaboration is based on the lecture notes in the course Combustion engines. (Valland(c) 2008) Dynamic state equations for open system approach can be described with five equations.

Gas equation

$$p * V = m * R * T \qquad (2.16)$$

Introducing the crank angle by logarithmic differentiation and solving for the gas constant gives:

$$\frac{1}{p}\frac{dp}{d\varphi} + \frac{1}{V}\frac{dV}{d\varphi} = \frac{1}{m}\frac{dm}{d\varphi} + \frac{1}{R}\frac{dR}{d\varphi} + \frac{1}{T}\frac{dT}{d\varphi} \qquad (2.17)$$

The expression for R differentiated to crank angle:

$$\frac{dR}{d\varphi} = \frac{\partial R}{\partial p} * \frac{dp}{d\varphi} + \frac{\partial R}{\partial T} * \frac{dT}{d\varphi} + \frac{\partial R}{\partial F} * \frac{dF}{d\varphi} \qquad (2.18)$$

The partial derivatives of R with respect to pressure and temperature are usually small. The terms will however be significant if dissociation is included (high temperature).

Combining the two equations and neglecting dissociation gives:

$$\frac{1}{p}\left[1 - \frac{p}{R}\frac{\partial R}{\partial p}\right] * \frac{dp}{d\varphi} - \frac{1}{T}\left[1 + \frac{1}{T}\frac{\partial R}{\partial T}\right] * \frac{dT}{d\varphi} - \frac{1}{R}\frac{dR}{dF} * \frac{dF}{d\varphi} - \frac{1}{m}\frac{dm}{d\varphi} + \frac{1}{V}\frac{dV}{d\varphi} = 0 \qquad (2.19)$$

Equation 2.19 is called the dynamic gas equation and represents the gas properties for variation in temperatures and pressure with respect to the composition and mass during the process.

The energy equation

The energy equation is based on the first law of thermodynamics for an open system. The total energy can be described by the following equation.

$$dU = dQ - dW + \sum h_i * dm_i \qquad (2.20)$$

The first term at the right side in equation 2.20 is the heat input, while dW is the actual working on the piston and the last term in the equation is related to the energy added or subtracted during fuel injection, exhaust stroke and air intake stroke. The flow velocity can be neglected due to its low value. The total energy is then equal to the internal energy.

Gas composition

The composition is defined by the fuel-air equivalence ratio from equation 2.7.

For a diesel engine, F will be close to and assumed zero during compression, will increase during combustion and will be constant during expansion.

Differentiating with respect to crank angle gives:

$$\frac{dF}{d\varphi} = \frac{1}{f_s} * \frac{df}{d\varphi} \qquad (2.21)$$

$$\frac{df}{d\varphi} = \frac{1}{m_A}\left[\frac{dm_F}{d\varphi} - f * \frac{dm_A}{d\varphi}\right] \qquad (2.22)$$

By identifying and rearranging the equation we can derive an expression for the dynamic mixing equation:

$$\frac{m}{1 + f_s F} * \frac{dF}{d\varphi} = \sum_i \frac{F_i - F}{1 + f_s F} * \frac{dm_i}{d\varphi} + \frac{1}{f_s} * \frac{dm_f}{d\varphi} \qquad (2.23)$$

F is constant during induction, compression, expansion, blow down and exhaust stroke.

The alteration in F can best be visualised in a three-dimensional diagram (PVF). An example is shown in figure 2. The diagram is not a result of dynamic cycle calculations, but a result from simple calculations based on end state conditions for each process.

Conservation of mass

The logic in this expression is that the change of mass in the system must be equal to the sum of mass flow into and out of the system.

$$\frac{dm}{d\varphi} = \frac{dm_{IV}}{d\varphi} - \frac{dm_{EV}}{d\varphi} - \frac{dm_{BB}}{d\varphi} + \frac{dm_f}{d\varphi} \qquad (2.24)$$

Flow leaving the system is flow through exhaust valve and gas blow. Flow entering is the air through the inlet valve and fuel flow.

Total volume

The volume in the combustion chamber is a function of the crank angle and can be described as follows:

$$V_C(\varphi) = V_d \left(\frac{1}{\varepsilon - 1} + \frac{1}{2} * \left[1 - cos\varphi + \left(\frac{1}{\lambda}\right)\left(1 - \sqrt{1 - (\lambda * sin\varphi)^2}\right) \right] \right) \qquad (2.25)$$

Differentiation of the volume function with respect of the crank angle gives the derivative function:

$$\frac{dV_c}{d\varphi} = \frac{V}{2}\left[sin\varphi + \frac{\lambda * sin\varphi}{2 * \sqrt{1 - (\lambda * sin\varphi)^2}} \right] \qquad (2.26)$$

Matrix notation

These five first-order differential equations describe the process in the combustion chamber in all two or four strokes. The different rows in the matrices represent the five previous described functions in the same sequence.

Dynamic state equations in matrix form:

$$
\begin{bmatrix}
\frac{1}{P}\left(1 - \frac{p}{R}\frac{\partial R}{\partial p}\right) & -\frac{1}{T}\left(1 + \frac{T}{R}\frac{\partial R}{\partial T}\right) & -\frac{1}{R}\frac{\partial R}{\partial F} & -\frac{1}{m} & \frac{1}{V} \\
m\frac{\partial u}{\partial p} & m\frac{\partial u}{\partial p} & m\frac{\partial u}{\partial p} & u & p \\
0 & 0 & \frac{m}{1 + f_s F} & 0 & 0 \\
0 & 0 & 0 & 1 & 0 \\
0 & 0 & 0 & 0 & 1
\end{bmatrix}
\begin{pmatrix}
\frac{dp}{d\varphi} \\
\frac{dT}{d\varphi} \\
\frac{dF}{d\varphi} \\
\frac{dm}{d\varphi} \\
\frac{dV}{d\varphi}
\end{pmatrix}
=
\begin{bmatrix}
0 \\
\frac{dQ}{d\varphi} + \sum h * \frac{dm_i}{d\varphi} + h_f * \frac{dm_f}{d\varphi} \\
\sum \frac{F_i - F}{1 + f_s F_i}\frac{dm_i}{d\varphi} + \frac{1}{f_s} * \frac{dm_f}{d\varphi} \\
\sum \frac{dm_i}{d\varphi} + \frac{dm_f}{d\varphi} \\
\frac{dV_c}{d\varphi}
\end{bmatrix}
$$

The left side represents the state variables and state vector while the right hand side represents interaction with the surroundings. This setup is beneficial when restrictions to the system are introduced. The dynamic state equations can give answers to parameters in the different processes depending on which parameters are known. For example flow rates in and out of the system, heat interaction, combustion duration, heat loss, accumulated heat release during combustion and crank angle at start of combustion can be determined based on measured cylinder pressure. Further specific fuel consumption, mean effective pressure, brake power, air consumption and volumetric efficiency can be determined if data on mechanical efficiency is known.

2.3.2. Complete dynamic engine analysis

In chapter 8 a complete engine model will be used to investigate influence of altering operating and fault conditions influence on the performance. A complete engine model can be simplified to reduce the need of input data and computation effort. Based on this engine models should be kept as simple and small as possible but still be sufficient to provide the necessary results. The dynamic process analysis is the most accurate analysis that can be performed for the diesel engine. Because of the complexity of the analysis computer program is necessary when performing these kind of analysis. This thesis will show that the results from a dynamic process analysis can be very accurate to real engine performance. Dynamic process analysis are therefore always used when designing and developing diesel engines.

3. Operating condition for ship propulsion engine

The propulsion engine for a ship will always be exposed to shifting operating conditions. The engine is tested at stable condition either on a test bed or at sea trials in calm water. In the following sections different conditions will be discussed regarding when they occur, the effect they impose on the engine and the consequences they bring along.

3.1. Added loads due to operation

A ships propulsion engine is normally specified for a ship with a given resistance through the water for a given draught. In new condition the engine has a margin that allows added loads relative to the new condition. This ensures that the engine does not operate outside the MCR for a given speed. Typical added loads and the impact on the engines operation will be discussed in chapter 3.1.1-3.1.5.

3.1.1. Wind

A ship in transit that encounters especially head wind will experience extra load to the engine to be able to maintain the service speed. Looking at the engine, the power required to maintain the desired shaft speed will be increased. The added resistance is dependent on the ships size and design. The added resistance for the ship caused by wind can be determined by simple models and input for wind speed, but is not a part of this thesis. The wind resistance is a relative stable added resistance to the total resistance of the ship. The wind load alone will rarely lead to reduction in speed to avoid overload but will have a small impact on the fuel consumption either positive or negative dependent on the relative wind direction compared to the ships course.

3.1.2. Wave

Waves are almost always present at open seas. Dependent on the ship and wave size the waves will involve fluctuating loads to the ships propulsion system. The situation inflicting the most fluctuation is stern seas, which is rather complex to calculate. As a consequence of heavy waves ships may have to reduce the speed to avoid overload of the engine.

3.1.3. Draught

The loading condition of the ship will give impact to the ships draught. The more cargo and/or ballast the larger draught and larger power demand for propulsion. The speed of the vessel and the fuel consumption in relation to sailed distance will depend strongly on this.

3.1.4. Manoeuvring

Manoeuvring for ships with two or more propellers will cause extra load to the propulsion-line which has the inner corner in the turning circle. This phenomenon is caused by the difference in water speed over the two propellers especially in sharp turns. This situation is not common for most ships but is relevant for military ships that performing rapid course changes.

Standard manoeuvring will also cause alterations to the load of the engine. This applies to all kinds of vessels. Heavy manoeuvring may for some vessels lead to short time overload to the engine. Most engine manufacturers allow overloading of the engine for shorter periods. From own experience the engine(s) may fail to produce the power required which leads to a drop in engine and ship speed. Manoeuvring will only have a minor impact on the fuel consumption, but may, for some ships, cause overloading of the engine.

3.1.5. Increased hull and propeller resistance

Over time the hull and propeller will be fouled with marine growth. This will increase the resistance and lead to increased demand of power from the propulsion engine to maintain the service speed of the vessel. The only way to cope with this is to regularly maintain the underwater surface of the ship and propeller by means of cleaning the hull and polishing the propeller. (MAN-B&W-Diesel-A/S 1998)

3.2.Ambient condition

The ambient conditions the ship encounters are always shifting. Engine performance is normally stated with ISO standard ambient conditions as reference. Deviating conditions from the standard conditions will affect the engine performance. The effects of changing ambient conditions for the Bergen Diesel KRG-6 engine will be estimated and simulated in chapter 8.

3.3.Part load and overload

A typical diesel engine has an efficiency or SFC function as shown in figure 5. Figure 5 is related to the load but engine speed vs. SFC will have similar shape. (Bergen-Diesel 1993)This implies that the best efficiency of a typical diesel engine is achieved at around 80% of load and speed. The propulsion engine gear and propeller should therefore be matched such that this point corresponds to the service speed of the ship. Operation far from this point will result in lowered efficiency. This fact is the main reason for the good efficiency obtained for diesel electric propulsion. The engines delivering the electric power can in such systems be operated close to this point for the whole speed range. However efficiency for a direct driven propeller operated at the best operating point is better than what can be obtained for diesel-electric system due to higher losses in the electric system than in a direct driven configuration.
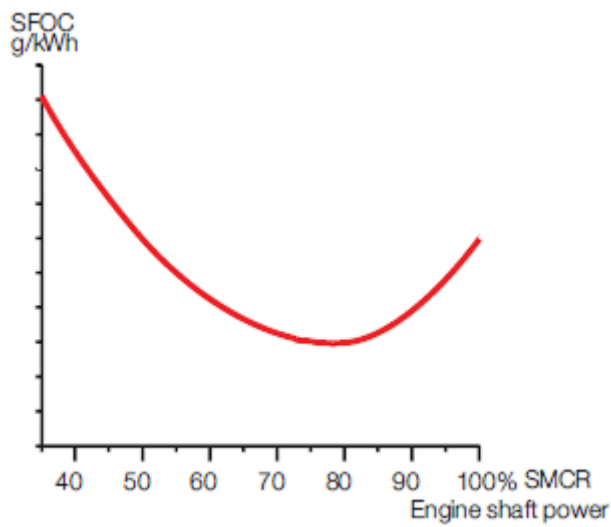
Figure 5 Typical SFC for a diesel engine(MAN-B&W-Diesel-A/S)

A ship in new condition operates along the standard propeller curve for the given ship and propulsion system configuration, but added resistance due to wave wind manoeuvring and draught will occur. A schematic propeller curve combined with typical engine load diagram is presented in figure 6. The propeller curve will shift either left or right dependent on the added loads to the ship. A heavy loaded ship i.e. large draught, with fouling on the ship's hull will move the propeller curve to the left in the diagram.
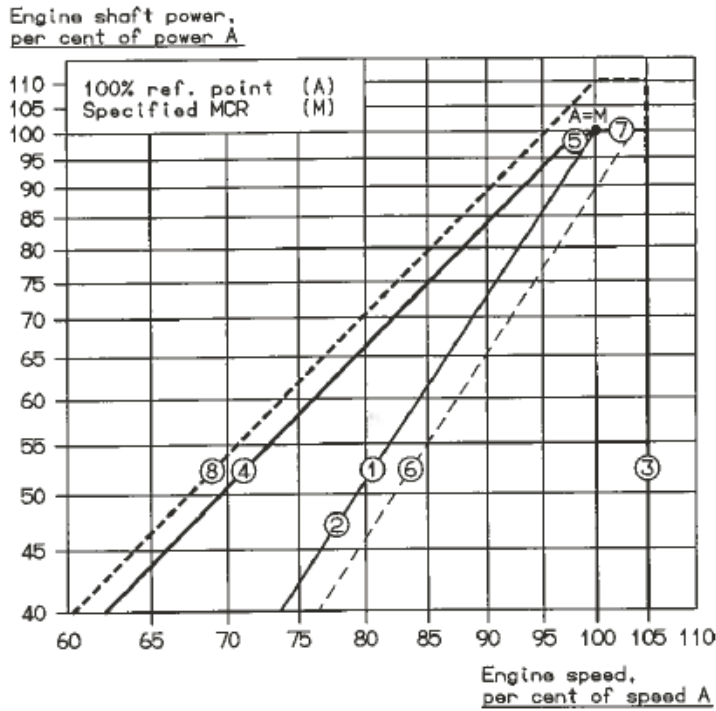
Line 1: Propeller curve through point A.
Line 2: Propeller curve - heavy running, recommended limit for fouled hull at calm weather conditions.
Line 3: Speed limit.
Line 4: Torque/speed limit.
Line 5: Mean effective pressure limit.
Line 6: Propeller curve - light running (range: 2.5-5.0%), for clean hull and calm weather conditions.
Line 7: Power limit for continuous running.
Line 8: Overload limit.

Figure 6 Propulsion engine load diagram(MAN-B&W-Diesel-A/S 1998)

To compensate for the added loads, fouling of the hull and the weather margins is usually implemented in the calculated propeller power. The extra power required to compensate for bad weather condition is called sea margin. Usually this margin is about 15% of the propeller design point. In addition an engine margin of 10% is normally added to compensate for fouling of the hull. Combined these margins will allow the ship to maintain the service speed without engine overload, providing that the added loads are not excessive. If these margins are not included reduction of engine speed is the only way to avoid overload of the engine. Long periods of overloading may lead to mechanical fatigue, while repeated overloading may result in thermal fatigue. (N.E Chell 1999)

3.4. Fuel quality

The fuel quality is essential to the engines performance. The quality of fuel can vary quite much between suppliers. When receiving fuel a datasheet is normally available so that the quality and content is known. A fuel sample is normally sent to a testing facility so that the quality is confirmed. This way adjustments and precautions can be taken to ensure good performance and limited wear of the engine related to fuel.(MAN-B&W-Diesel-A/S 1998) The theory will not be detailed her but main topics regarding the fuel quality will be highlighted.

3.4.1. Heating value

The heating value indicates the amount of heat that is "stored" in a kg fuel. Normally the heating value is given assuming that the water content is vapour. The condensation heat is therefore not included. This heating value is known as the lower heating value (LHV). The LHV is nearly only determined on the carbon/hydrogen ratio, which is almost uniquely fixed by the density. This leads to the conclusion that more fuel is needed if the heating value is reduced to produce the same amount of heat release during combustion. Normally diesel engines running on heavy fuel are de-rated to allow for all kind of adverse conditions that are associated with heavy-fuel combustion. As a consequence the efficiency can be somewhat lower. (Stapersma 2009) The Bergen diesel engines in the K series should be de-rated by 10% in engine power when operating on heavy fuel.(Rolls-RoyceMarineAS 2001)
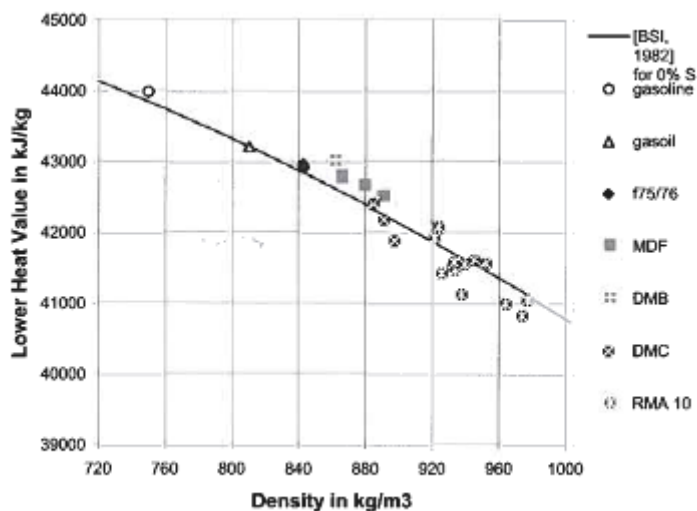
Figure 7 Plot of NO formation in a typical diesel engine(Stapersma 2009)

3.4.2. Ignition Properties

Diesel engines operate by self-ignition of the injected fuel. The fuels ignition property is therefore important for the combustion process. The short delay between injection and ignition is known as the ignition delay. In case of an extended delay more fuel is injected and premixed before ignition occur. This will cause an increase in steepness of the pressure rise and is known as "diesel-knock". Diesel knock can in extreme cases lead to engine damage. The combustion will to some extent be completed later in the engine cycle.

Supplied data for fuel oil does normally not contain details about the ignition quality. The Ignition quality can to some extent be predicted by calculations based on viscosity and density. This is calculated by formulas developed by the oil industry; e.g. Calculated Carbon Aromaticity Index (CCAI). High density combined with low viscosity may indicate poor ignition quality. (Stapersma 2009)

3.5. Fault conditions

A diesel engine will over time be worn and the condition for the various components will be reduced relative to the new condition. The fault conditions, which will be further analysed in chapter 8, are:

- Compressor condition
- Turbine condition
- Charge air cooler condition
- Injection timing

Some other typical faults are:

- Injector fault (bad spray, or leaking)
- Excessive pressure drop in charge air cooler
- Excessive pressure drop in exhaust pipe and muffler
- Compression fault
- Valve faults (gas leak)
- Air filter excessive pressure drop

Generally all faults will impose negative effect to the performance of the engine. Depending on the seriousness of the fault, reduction in power and speed might be necessary and in extreme cases the engine will have to be shut down.

4. ISO reference conditions and corrections

Engines are normally designed and tested according to ISO standard reference conditions. These conditions are stated in ISO 15550.

Air temperature	T_{ra}	298	K
Total barometric pressure	p_{ra}	100	kPa
Relative humidity	$ø_{ra}$	30	%
Charge air coolant temperature	T_{cra}	298	K

Table 2 ISO reference conditions

Engines in marine applications often operate in fluctuating ambient conditions. The conditions the ship is operating in must be known so the manufacturer can do the necessary adjustments in order to make the engine able to meet the requirements to power output and service intervals. International standard organisation has made standards that states how the engine performance should be measured during factory tests and also provided a calculation method for determining non-reference conditions engine performance. The intention of these calculations is to determine the max continuous rating the engine should be allowed to operate in without exceeding limits such as exhaust temperatures and turbine speed. The calculation methods are stated in ISO 3046-1. Non reference calculations for increased specific fuel consumption due to altered ambient conditions are also incorporated. Different types of engines react different to changes in ambient condition. ISO 3046 differentiate between engines based on principle and equipment such as Otto vs. Diesel principle and turbo charged vs. no turbocharged engines, which makes the calculations more realistic. The calculations are of course just an approximation which can be used if the engine manufacturer does not have data for the non reference conditions in question.(ISO-3046-1 2002) The intention of looking into this ISO-correction procedure here is to compare calculated and the simulated fuel consumption.

4.1.Power adjustment for ambient conditions for the KRG-6

If a turbo charged engine has not reached the limits of turbo charger speed, turbine inlet temperature and maximum cylinder pressure at declared power under standard reference conditions, the manufacturer can declare substitute reference to or from which power adjustment shall be made(ISO-3046-1 2002). This means that the engine is capable of producing more power than specified when the engine operates at standard reference condition.

The power is corrected by the following equation

$$P_x = \alpha * P_{ra} \tag{4.1}$$

The power adjustment factor α is given by the following expression:

$$\alpha = k - 0,71(1-k)\left[\frac{1}{\eta_m} - 1\right] \tag{4.2}$$

η_m is the mechanical efficiency. If the mechanical efficiency for the engine is unknown $\eta_m = 0,8$ according to ISO 3046-1 10.3.3. is to be used.

$k$is the ratio of indicated power and is described by the following equation:

$$k = \left(\frac{P_x}{P_{ra}}\right)^m \left(\frac{T_{ra}}{T_x}\right)^n \left(\frac{T_{cra}}{T_{cx}}\right)^s \tag{4.3}$$

Where the substitute reference total barometric pressure is:

$$P_{ra} = P_r \left(\frac{r_r}{r_{r,max}}\right) \tag{4.4}$$

The factor *a* and exponents *m, n, s* have numerical values given in the standard. For a turbo charged engine with charge air cooling these are set to be a=0 m=0,7 n=1,2 and s=1 ref. (table 2 in ISO-3046).

The KRG-6 engine is able to develop the stated power of 1165KW at the non reference condition stated in table 3 since the limits are not met,(Rolls-RoyceMarineAS 2001) and power adjustment calculations are therefore not performed.

4.2. Recalculation of fuel consumption for KRG-6

The specific fuel consumption will increase relatively to the standard conditions because of the altered ambient condition. The increase in specific fuel consumption can be approximated utilizing calculation routines from ISO-3046.

Air temperature	T_x	308	K
Total barometric pressure	P_x	100	kPa
Relative humidity	$\emptyset_x$	30	%
Charge air coolant temperature	T_{cx}	298	K

Table 3 Non-reference condition for comparison

In this calculation the engine is operating at 720rpm and 100% load.

The new SFC is found by multiplying t with a coefficient β:

$$b_x = \beta b_r \qquad (4.5)$$

Where $\beta = \dfrac{k}{\alpha}$

k and α is described in equation 4.2 and 4.3.

Calculations based on ISO 3046 give the engine a SFC of 197,5/kWh (0,5 g/kWh increase) for the non-reference condition stated in table 2 (ref appendix 1 for calculations). The results from this recalculation of fuel consumption will be compared with results from simulations in GT power. This comparison can be found in the chapter 8.4.5.

5. Diesel engine performance analysis motivation

The diesel engine is today the most common power generating engine used for both propulsion and auxiliary power generation onboard a ship. The engine represents a large investment cost when a new ship is built. During the service life of a ship the engines is accountable for a large portion of the ship voyage costs related to fuel /lubrication oil consumption and operating costs related to maintenance. It is therefore very interesting to investigate how the ships engine will react to altering operation conditions such as ambient conditions and fault conditions. The altering conditions will result in performance deviating from the engine's new condition performance and might cause thermal overload and excessive wear to exposed engine components. This altered performance will in most situations result in a larger fuel consumption which will cause increased voyage costs for the ship owner. The altered condition might also cause increased NO_x emissions which today are regulated and taxed. The ship owner is of course interested in keeping the operating and voyage costs as low as possible. Performance analysis can provide answers regarding how altered operating conditions will cause increased costs and further be used as important input data when deciding which measures needs to be taken. An example is shown in chapter 9, where the effect of reduced turbo charger effectiveness to a 2-stroke diesel engine is investigated. Performance analysis is also used by engine developers. This is however on a very detailed and complex level.

Modern diesel engines rely on several sub systems. Each of these subsystems can inflict a large impact on the engine's overall efficiency and emission discharge. For naturally aspirated engines the relation between change of ambient and fault conditions are straight forward. When a modern 2 or 4 stroke turbo charged and charge air cooled diesel engine is to be analysed the analysis is much more complex. The largest problems occur when trying to analyse fault conditions for these kinds of engines. Altered performance due to changing ambient conditions can be estimated rather easily based on ISO standards as shown in the previous chapter. The accuracy from such estimations is good, but not exactly the same as the comparison in chapter 8.4.5 shows.

The dimensioning parameter for an engines power and torque when its dimensions are set is the charge air density. The density and volumetric efficiency determines the amount of fuel that can be burned. This is limited to the point where a good combustion seas to occur, to high fuel/air ratio. The modern diesel engines charge air density level is limited to its BMEP and max pressure during combustion due to material stress. (Heywood 1988) Ambient condition analysis relates to the density of the charge air for the engine and cooling water temperature. It can therefore be generally estimated such as in the ISO standard. As mentioned this is only an estimate. A simulation of the actual engine will be able to provide more accurate results.

Ambient condition performance analysis can be valuable when:

- accurate determining max allowed rating for different ambient condition
- discussing if extra measures should be taken so that the engine can operate without restrictions
- varying ambient conditions effect on the engine

Such determinations can also be done based on actual measurements on the engine, but this is very often expensive and undesirable or even impossible to do.

Fault conditions for a supercharged diesel engine can be difficult to determine directly from classic measurements done by engine operators. Performance analysis can provide knowledge on how component faults will give impact on the engines overall performance and key parameters. An engine operator can then compare simulated engine trends for different fault conditions towards the measurements performed on-board. This will provide a sensible and good decision background when maintenance shall be planned. Engine operation with a faulty component will almost in all situations result in increase of SFC. To avoid thermal overload of exposed components it might also be necessary to reduce the mean effective pressure for the engine.

6. Performing an analysis

A turbocharged engine thermo dynamical model can be broken down in the following sub-models:

- Compressor (and air filter)
- Air cooler
- Flow in pipes
- Flow through inlet valve
- Air motion in the cylinder (swirl)
- Dynamics in the injection system
- Fuel jet interactions during diesel injection
- Combustion, including determination of products
- Noise generation
- Heat flow in combustion chamber
- Turbine

These are general sub-models. It might be necessary to model other processes depending on what results the model and analysis should provide. The model outlined above and in figure 8 is a thermodynamic model. This means that the mechanical part of the engine is not included. The engine mechanical model can be introduced if the results require it. (Stone 1999)
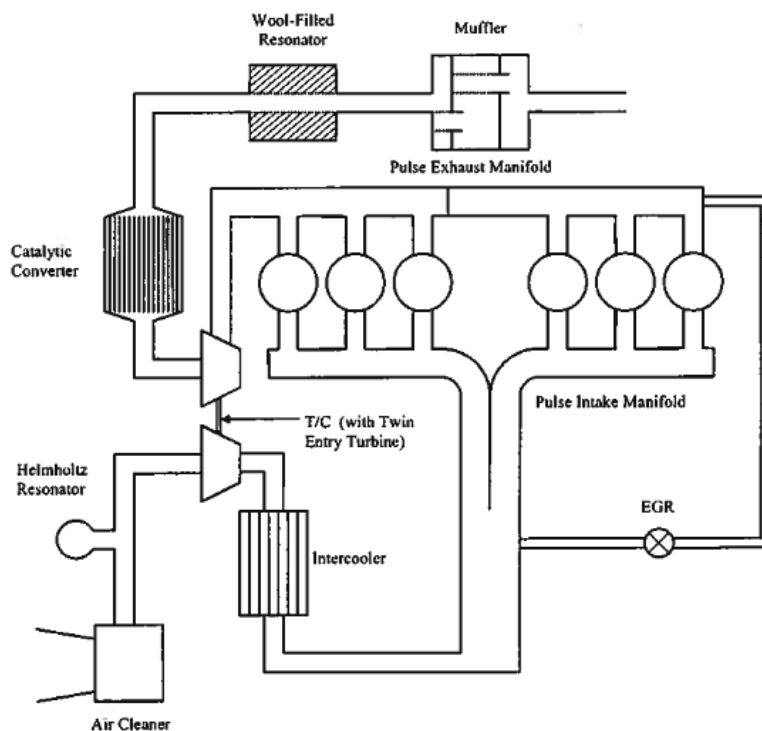
Figure 8 Basic engine with air supply and exhaust systems

 When building a dynamic simulation model in GT-POWER the following list of data is generally good starting point in requiring data needed. In this thesis the approach is to use a model of an existing engine. This means that the data needed exists and can be gathered.

Engine characteristics:

Compression ratio, firing order, inline or V-configuration, mechanical efficiency

Cylinder geometry:

Bore, stroke, connection rod length, pin offset, piston TDC clearance height, head bowl geometry, piston area and head area.

Intake and exhaust System:

Geometry of all components such as manifolds, runners, ports, catalysts, tailpipe and mufflers. Coefficients for head loss. Head loss can optionally be stated in terms of a coefficient.

Fuel injection:

Location of injectors, number of nozzle holes and nozzle diameter (sac volume)type of fuel, injection timing.

Intake and exhaust vales

Valve diameter, lift profile, discharge coefficient, valve lash, swirl coefficient and tumble coefficient.

Turbocharger

Turbine and compressor maps, turbo performance at several engine operating points.

Ambient state

Pressure, temperature (coolant and air) and humidity.

After the model has been built it is beneficial to compare simulation data to actual measured data. This way the model can be calibrated. Relevant measured data are:

- Power, brake torque
- Motoring friction power
- Air flow, fuel flow, air fuel ratio
- IMEP, BSFC, volumetric efficiency and air consumption
- Turbocharger speed
- Cylinder pressure and/or combustion rate
- Dynamic intake pressure
- Dynamic exhaust pressure
- Intake and exhaust manifold pressure and temperature
- Mean temperature at exhaust ports, entrance of the takedown pipe
- Exhaust wall temperature

Calibration is a iterative process where inputs are adjusted to obtain the best compliance between measured and simulated data.(GammaTechnologies 2006)

6.1. GT-power simulation aspects

A simulation program such as GT-POWER let the user choose amongst several sub-models such as heat flow models and combustion models, to simulate the cylinder cycle. Important choices of such are outlined in the following subchapters.

6.1.1. Products of combustion

GT-power is initially set up to predict the following products of combustion based on equilibrium chemistry:

- N_2
- O_2
- CO_2
- CO
- H_2O
- H_2
- H
- O
- OH
- NO
- N

Selected species may be calculated by chemical kinetics, but only for certain combustion models. Combustion models are discussed in chapter 6.3.

NO_x

All combustion models in GT-POWER have the capability to calculate NO_x concentration. GT-POWER uses the extended Zeldovich mechanism to compute the NO_x formation in a diesel engine. This means that only thermal NO is calculated by the program. The results are very sensitive to the trapped cylinder mass, fuel-air ratio and combustion rate. Temperature is also very important and therefore a two zone temperature model should always be used instead of single zone, when NO_x predictions shall be performed. The combustion model used in the KRG-6 engine simulation is a non-predictive combustion model. This means that it relies on a predefined burn rate. The simulation model uses a two zone combustion model, one burn and one unburned zone (GammaTechnologies 2006).

The model has been calibrated to the engine shop trials regarding NO_x emissions. The numbers obtained from the shop trials are too low for this engine. Instead of using the brake specific NO_x results from GT-POWER, a trend based on percentage alteration is used when presenting the results.

6.1.2. Speed vs. load mode

GT-POWER can be set up to run in both modes, but speed mode is the most commonly used mode for engine simulation. A constant speed is imposed to the program and the simulation will typically provide a steady state result. Setting the speed from the beginning provides very quick results, eliminating the long period of time that a loaded engine would requires to reach steady state. Speed mode will be used for the simulation of the KRG-6 engine.

In load mode a load can be imposed to the engine, and the speed is then calculated by the predicted brake torque of the engine, the load torque and the engine inertia. Load mode can be used to retrieve information on the engines response to load. The nature of these simulations requires many simulations to provide the desired results. It is common to build and calibrate the model using speed mode and later use load mode to retrieve the desired results for load response from the engine(GammaTechnologies 2006).

6.2. In cylinder heat transfer

The in cylinder heat transfer can be calculated based on one of the following options:

- **Modified Woschni model**
  Heat transfer in cylinder modelled after the Woschni model is a well know and used model in engine simulation and will not be elaborated on here. It is often noticed during engine simulation that the Woschni model under predict the heat transfer in the engine cylinder. This problem is corrected by using a convection multiplier.

- **Hohenberg model**
  This model is similar to the Woschni model, but has shown to be more accurate especially for direct injection diesel engines with high cylinder and charge air pressure. This model is used for the simulation of the KRG-6 engine.

- **Flow model**
  The heat transfer is modelled based on the flow of the gases in the cylinder. An efficient velocity is calculated based on radial and axial velocity, swirl, tumble, turbulence intensity and turbulence length. Based on this velocity a heat transfer coefficient is determined.

- **Hg profile model**
  A heat transfer coefficient is imposed to the program by an array defined by the crank angle. The coefficient must then be pre determined by from a separate calculation.

- **User defined model**
  A user defined model can also be used.(GammaTechnologies 2006)

6.3. Combustion model

GT-POWER divides the combustion models available in the program between predictive and non-predictive models. The non-predictive models impose a burn rate as a function of crank angle. This burn rate will be used regardless of condition in the cylinder. Therefore the burn rate will not be affected by factors such as residual fracture or injection timing. Non-predictive combustion models should therefore be used when studying variables that have little effect on the burn rate. There are several non-predictive models in the program used for diesel engine combustion:

- **Imposed combustion profile**
  A burn rate profile can be directly imposed as a function of crank angle. This method is particularly useful if the in-cylinder pressure has been measured in a laboratory, since the burn rate can be calculated from the cylinder pressure.

- **Direct-injection diesel Wiebe model**
  This method imposes the burn rate for direct-injection diesel engines by utilizing a three-term Wiebe function. The Wiebe curves approximate the typical shape of the burn rate for this type of engine. The purpose of using triple Wiebe function is to be able to separate the three phases during combustion; the premixed, mixing controlled combustion and the late combustion phase. This model can provide a reasonable burn rate if the cylinder pressure is not known. This model is used for the simulation of the KRG-6 engine.

- **Multi Wiebe model**
  The model is similar to the previous but instead of triple, multiple Wiebe functions are used to describe the burn rate. The main use of this model is to model burn rate when several injection events are used.

There is only one predictive combustion model for diesel engines included in the program.

- **Direct injection Diesel jet model**
  This model can only be used for direct-injection diesel engines. It is intended for prediction of burn rate and NO_x emissions. The injected mass is divided into five radial zones and a maximum of 80 axial zones. At each time step during the injection period an axial slice is injected into the cylinder. The total mass of fuel in the zones is equal to the specified injection rate divided by the number of nozzle holes. Each zone is divided into four sub zones. When a zone is injected with fuel it is 100% full of fuel. As the zone moves into the cylinder the fuel evaporates and converts to an unburned zone consisting of air and fuel. The fuel-air ratio can be determined based on the size of the zone. The temperature of the zone can then be determined based on the air temperature, fuel temperature and the evaporation energy. When the combination of cylinder pressure, zone temperature, and fuel air ratio becomes combustible, the zone transfers to a burned zone. The temperature and composition can then be determined. NO_x formation is calculated for each zone based on temperature and air fuel ratio in the zone. Total NO_x formation in the cylinder is determined by summarising the concentration in all the burned zones(Hatlevold 2009).

7. NO$_x$ formation in compression ignition engines

NO$_x$ is an abbreviation for nitrogen oxides and comprise both NO and NO$_2$. Four different mechanisms lead to the formation of NO$_x$ in the combustion chamber; thermal NO, prompt NO, fuel NO and intermediate N$_2$O. Thermal NO is formed at high temperature at slightly lean conditions within the burned gas. The reactants forming thermal NO stems from the combustion air. Prompt NO describes the reaction of N_2 from the air and the hydrocarbon radicals in the fuel-rich zones. The reaction takes place in the combustion zone because of the need of hydrocarbons. The fuel NO refers to the formation of NO from fuel bound nitrogen. Intermediate N$_2$O is formed at lower temperature than the thermal NO in fuel-lean and high pressure environment. This fourth mechanism has a minor effect in the diesel engine. From studies performed on NO$_x$ formation in diesel engines it is widely known that thermal NO contributes to 80-95% of the NO$_x$ emission. Therefore NO$_x$ estimations from simulations and calculations are often solely based on thermal NO formation (G.Stiesch 2003).

7.1.1. Formation of thermal NO

The formation of NO_x from thermal NO is described by the extended Zeldovich mechanism. It describes the break out of a nitrogen molecule by an oxygen atom, and subsequent oxidation of the nitrogen atom. The mechanism contains the tree following equilibrium reactions:

$$O + N_2 \Leftrightarrow NO + O \quad k_{i,f} = 7.6 * 10^{13} \exp^{\left(-\frac{38000}{T}\right)} \tag{7.1}$$

$$N + O_2 \Leftrightarrow NO + O \quad k_{ii,f} = 6.4 * 10^9 \exp^{\left(-\frac{3150}{T}\right)} \tag{7.2}$$

$$N + OH \Leftrightarrow NO + H \quad k_{ii,f} = 4.1 * 10^{13} \tag{7.3}$$
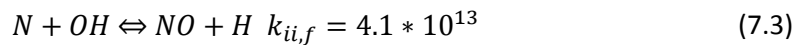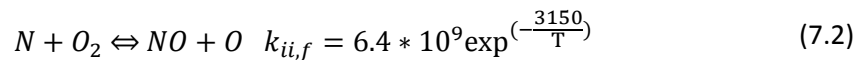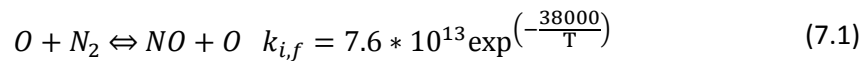
k_- is the rate constant of the reaction and describes the reaction rate for a given temperature. These reaction rates have been measured in numerous experimental studies(Heywood 1988). Thermal NO has got its name because of the first reaction mechanism, which initiates the overall mechanism by production of nitrogen atoms. The first reaction proceeds only at high temperatures. This is obvious from the high activation energy required. Large amounts of NO are consequently produced only in the hot burned gas zones with temperature above 2000 K. This is why the reaction path is called thermal NO. The reactions require time to reach chemical equilibrium and since the time window of thermal NO production in a diesel engine is relatively small, (especially for medium and high speed diesel engines)equilibrium is not met (G.Stiesch 2003).

After the start of combustion, the increase in the NO concentration falls behind the ideal equilibrium because the slow chemistry cannot follow the fast increase in gas temperature due to combustion. Later in the engine cycle the equilibrium NO concentration decreases almost to zero because gas temperature is reduced again during the expansion stroke. However, the realistic NO concentration does not follow its equilibrium value. It rather "freezes" at a concentration much greater than the equilibrium value corresponding to exhaust condition. This freezing of the reverse reactions of the mechanism is partly caused by the temperature dependence of the respective rate coefficients, and partly, because the concentration of the N-, O-, and H-atoms, that are necessary for the reverse reactions to proceed, are drastically reduced when the temperature decreases during expansion(G.Stiesch 2003).

Because of the time required and freezing, the NO formation in diesel engines has to be estimated by a rate controlled process

The forward and reverse rate coefficients (k_i^+ and k_i^-) for the reactions in equation 7.4 have been tested and measured in several experiments. Based on that, recommended values have been determined. The formation of NO can be determined by:

$$\frac{d[NO]}{dt} = k_1^+[O][N_2] + k_2^+[N][O_2] + k_3^+[N][OH] - k_1^-[NO][N] \tag{7.4}$$
$$- k_2^-[NO][O] - k_3^-[NO][H]$$

[-] denotes the species concentration.

k_1^+, k_2^-, k_3^- require large activation energy which is the reason for the strong temperature dependence for NO formation. In Heywood it is explained like this:

NO forms in both the flame front and the post flame gases. In engines, however, combustion occurs at high pressure so the flame reaction zone is extremely thin and residence time in the zone is short. Also, the cylinder pressure rises during most of the combustion process, so burned gases produced early in the combustion process are compressed to a higher temperature than they reached immediately after combustion. Thus, NO formations in the post flame gases almost always dominate any flame front-produced NO. It is therefore appropriate to assume that the combustion and NO formation processes are decoupled and to approximate the concentration of O, O_2, OH, H, N_2 by their equilibrium values at the local pressure and equilibrium temperature.(Heywood 1988)

This can be modelled with the following equation:

$$\frac{d[NO]}{dt} = \frac{6 * 10^6}{T^{0,5}} exp\left(\frac{-69,090}{T}\right)[O_2]_e^{0,5} * [N_2]_e \tag{7.5}$$

Figure 9 shows plots for NO formation during 5.6 ms for several values of oxygen concentration, cylinder pressure and a comparison with the NO equilibrium equation. The figure shows that NO formation does virtually not occur beneath 2000°C and that it rises steeply from there, but is still well below the equilibrium line. The mean bulk temperature in a diesel engine does generally not exceed 2000°C. This proves that local high temperature zones are responsible for NO formation in the diesel engine (Hatlevold 2009).
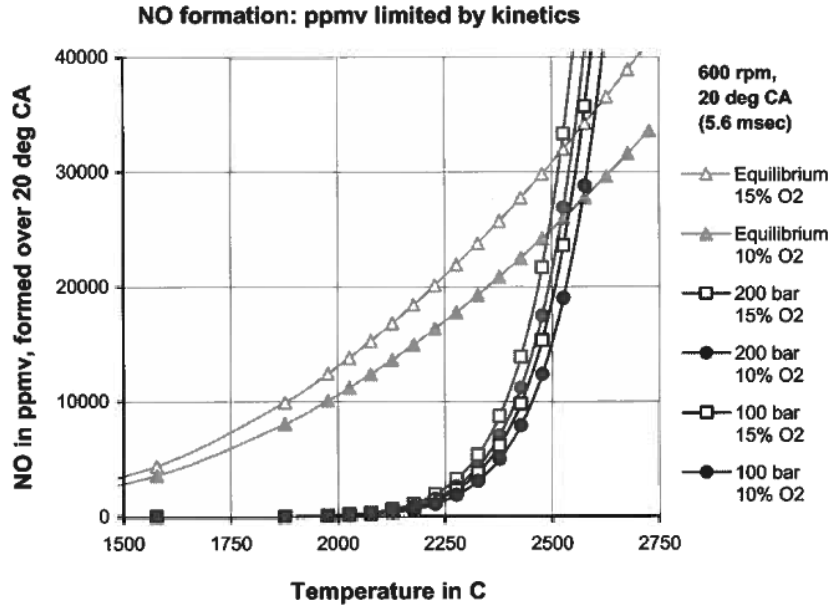
Figure 9 Plot of NO formation in a typical diesel engine(Stapersma 2009)

7.1.2. Formation of prompt NO

Formation of prompt NO was first described by C.P. Fenimore and is therefore referred to as the Fenimore mechanism. Prompt NO is formed directly within the reaction zone. The reaction is more complex than the reactions forming thermal NO. The rate-limiting step in the mechanism is the reaction of CH radical with molecular nitrogen to hydrocyanic acid and a nitrogen atom.(G.Stiesch 2003)

$$CH + N_2 \rightarrow HCN + N,$$
$$k_f = 4.4 * 10^{12} \exp\left[-\frac{11,060}{T}\right] cm^3/(mol\ s) \tag{7.6}$$
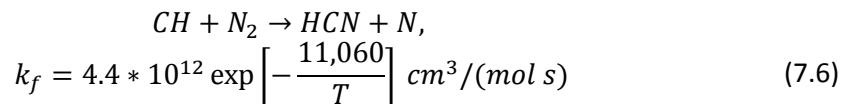
The free nitrogen atom can further be converted to NO by the second and third extended Zeldovich mechanism. The HCN further reacts with other compositions in the combustion chamber to form NO via the intermediate NCO. There are many reactions that contribute to this NO formation, some are:

$$HCN + OH \rightarrow CN + H_2O \tag{7.7}$$

$$CN + O_2 \rightarrow NCO + 0 \tag{7.8}$$

$$HCN + O \rightarrow NCO + H \tag{7.9}$$

$$NCO + O \rightarrow NO + CO \tag{7.10}$$

$$NCO + OH \rightarrow NO + CHO \tag{7.11}$$
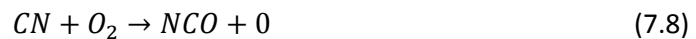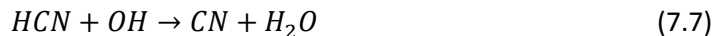
A complete list identified by Fenimore can be viewed in figure 9.

This actual mechanism is more complex than thermal NO mechanism since more reactions and intermediate species are involved. Some aspects are worth noticing regarding prompt NO_x. *Since the rate-limiting reaction step in equation 7.6 involves the CH radical, the prompt NO path becomes*

31

*important only during fuel rich condition where noticeable CH concentrations can be detected. (G.Stiesch 2003)*The activation energy for prompt NO is far less than for the thermal NO. This means that prompt NO formation is not as dependent on high temperature as thermal NO. As a consequence prompt NO formation becomes more prominent for combustion at lower temperature. The rate coefficient for prompt NO is more uncertain than the ones for thermal NO. Therefore the estimation of prompt NO is less accurate than estimations for thermal NO. It is also complex to determine the CH concentration in the flame zone.

The uncertainties and complexity of prompt NO estimation mentioned above is the main reason that this contributor to the total NO_x emission is excluded in most studies and simulation programs. In addition the contribution is relatively small compared to the thermal NO formation.

7.1.3. Formation of NO_2

Normally NO_2 would be negligible compared to the concentration of NO during and after the combustion, but tests show that NO_2 contributes to 5-10% of the NO_x emission from a diesel engine.

Mechanism for NO_2 formation:

$$NO + HO_2 \Rightarrow NO_2 + OH \qquad\qquad (7.12)$$

Normally the NO_2 would convert into NO as long as there is enough oxygen present and the temperature is high enough. This mechanism can be described with the following reaction:

$$NO_2 + O \Rightarrow NO + O_2 \qquad\qquad (7.13)$$

Mixing products with cooler air can quench the reaction from NO_2 to NO and is the reason for the relatively high concentration of NO_2 (Stapersma 2009). The quenching is dominant for diesel engines at light load due to the relatively large amount of cool air in the combustion chamber (Cool regions)(Heywood 1988).

7.1.4. Formation of intermediate N_2O

NO_2 is not a dominating part of the reaction products from combustion. Specialized literature on the subject states that about 1% of the NO amount is converted to N_2O in the exhaust (Stapersma 2009). This contributor is therefore not elaborated further.

7.2.General NO_x formation theory for compression ignition engines

The fuel-air mixing and combustion in a diesel engine is extremely complex. The injection of fuel starts just before the combustion starts. A non-uniform combustion gas temperature and composition is the result from a non-uniform fuel distribution through the injection and combustion phase. The combustion is normally parted into two phases; premixed phase and the mixing-controlled phase. During the premixed phase the combustion spread close to stoichiometric due to spontaneous ignition and flame propagation. During the mixing-controlled phase the burning mixture is likely to be closer to stoichiometric combustion. In addition to these two different combustion phases the temperature and pressure in the combustion chamber is shifting due to the movement of the piston. NO_x is mainly formed in the high temperature region just after start of the combustion and max peak pressure. Max temperature lags the max pressure in the combustion chamber. The decreasing temperature due to expansion and mixture between unburned and burned gas will freeze the NO chemistry early in the expansion process, and a minor decomposition of NO occurs.

Results from cylinder-dumping tests show that most of the NO is formed within the first 20 deg after combustion starts. If injection timing is retarded the combustion process also will be retarded. Max pressure and temperature during the combustion will be lower. As NO formation is strongly dependent on high temperature a retardation of ignition timing will result in lower NO formation.

EGR (exhaust gas recycle) is a method used to reduce the NO formation in combustion engines. Exhaust gas heat capacity is higher than air. And the excess of oxygen is reduced. These two factors result in a decrease of NO_x emission when this technology is used.

EXTENDED ZELDOVICH MECHANISM - (THERMAL NO)	
$N + O_2 \rightarrow NO + O$	$NO + OH \rightarrow NO_2 + H$
$N + OH \rightarrow NO + H$	
NO VIA N_2O	
$CO_2 + N \rightarrow NO + CO$	$N_2O + OH \rightarrow N_2 + HO_2$
$N_2O + O \rightarrow N_2 + O_2$	$N_2O + M \rightarrow N_2 + O + M$
$N_2O + O \rightarrow NO + NO$	$N + NO \rightarrow N_2 + O$
$N_2O + H \rightarrow N_2 + OH$	
FENIMORE MECHANISM - (PROMPT NO)	
$NO + HO_2 \rightarrow NO_2 + OH$	$NCO + NO \rightarrow N_20 + CO$
$NO + O_2 \rightarrow NO_2 + O$	$NCO + H_2 \rightarrow HNCO + H$
$NO + NH \rightarrow N_2O + H$	$CN + O_2 \rightarrow NO + CO$
$CH_2 + N_2 \rightarrow HCN + NH$	$CN + O_2 \rightarrow NCO + O$
$CH + N_2 \rightarrow HCN + N$	$CN + OH \rightarrow NCO + H$
$CN + N \rightarrow C + N_2$	$CN + O \rightarrow CO + N$
$HCN + OH \rightarrow CN + H_2O$	$CN + NO \rightarrow CO + N_2$
$HCN + 0 \rightarrow NCO + H$	$NH + OH \rightarrow N + H_2O$
$HCN + O \rightarrow NH + CO$	$NH + H \rightarrow N + H_2$
$HCN + O \rightarrow CN + OH$	$NH + O_2 \rightarrow NO + OH$
$NCO + H \rightarrow NH + CO$	$NH + NO \rightarrow N_2 + OH$
$NCO + O \rightarrow NO + CO$	$C + NO \rightarrow CN + O$
$NCO + N \rightarrow N_2 + CO$	$HNCO + H \rightarrow HCN + OH$
$NCO + OH \rightarrow NO + CO + H$	$HNCO + OH \rightarrow NCO + H_2O$
$NCO + M \rightarrow N + CO + M$	$CH_3 + NO \rightarrow HCN + H_2$

Figure 10 Fraction of frozen NO from combustion (Ken-ichi Kohashi 2003)

The work performed by Ken-ichi Kohashi et al. 2003 proves that almost 90 % of the NO_x emissions from a diesel engine are related to the thermal NO mechanism (Extended Zeldovich mechanism). The other contributors are the prompt NO formation which is responsible for app. 7 % and the NO from N2O relations with approximately 1,5%. The rest of the NO produced is gathered in an "other category" which hasn't been successfully described. Since NO from Fenimore mechanism is rather difficult to compute and the two other small contributors are very small compared to the thermal NO formation, these three contributors are often neglected when performing NO_x simulation calculations (G.Stiesch 2003).

8. Ambient and fault conditions introduced in engine simulation
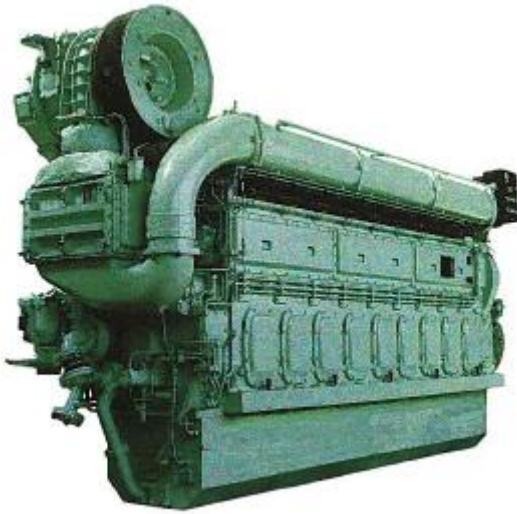
Figure 11 Illustration of the K-type engine

8.1. Background

The background for these simulations is the project work performed in the fall semester 2009. Impacts from changing operating and ambient conditions were identified and described. In this chapter the changing ambient and fault conditions will be investigated closely by introducing these in to a simulation model for a Bergen Diesel KRG-6 engine. The simulation model is built by Bergen diesel and calibrated by PhD. Nabil Al Ryati at Marinteknikk, NTNU, Trondheim. Further modifications and calibrations have been made to the model.

8.2. Engine description

Bergen Diesel K-type diesel engine is a four stroke engine built in both Vee and in-line configuration. It has 250mm stroke and 300 mm stroke. The engines are turbocharged and based on impulse principle. The engine is equipped with a two stage charge air cooling system. The engines are manufactured as propulsion (KRM or KVM) and generator engines (KRG or KVG). The engines can be equipped to operate on heavy fuel of viscosity up to 700 cSt at 50$^{\text{o}}$C (Rolls-RoyceMarineAS 2001). The engine that will be simulated here is the Bergen diesel KRG-6 generator engine (K-type of engine, R-inline, G-generator engine, 6-cylinders).

The simulation model used is a model including all engine components that affect performance of the engine. Cooling water system and oil systems are not included but these are not needed for this kind of study.
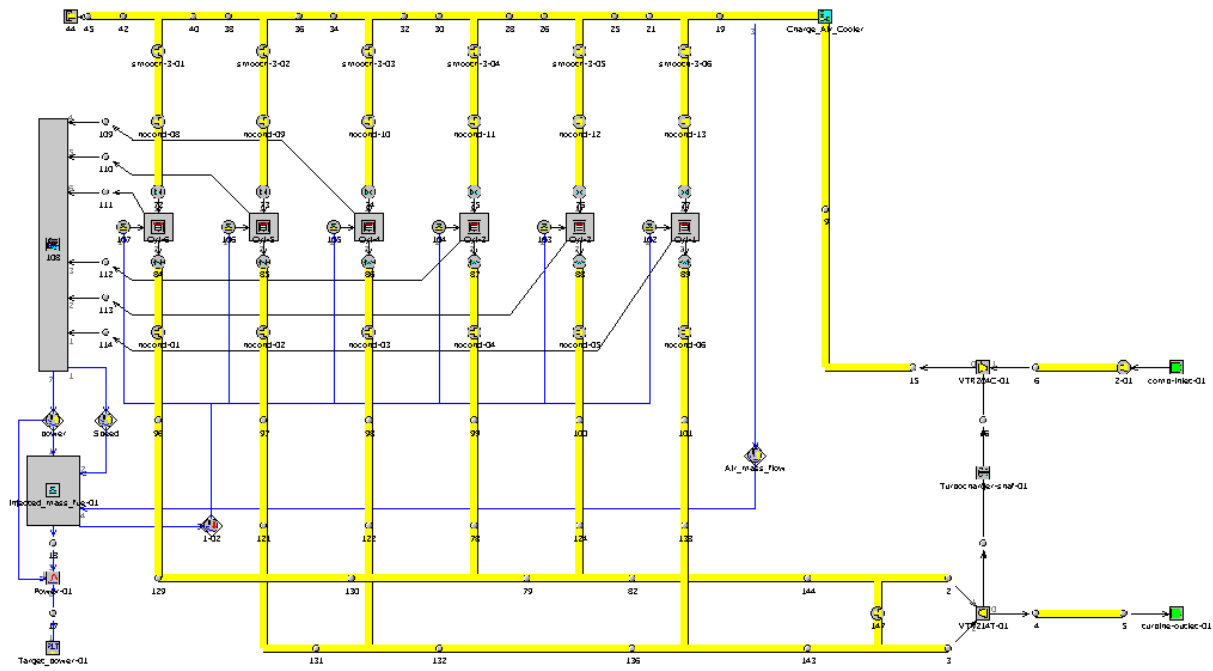
Figure 12 GT-Power model of the KRG-6 engine

The yellow lines in figure 12 represent the air and exhaust flow through the engine. The gas path starts and ends in an environment template stating the ambient conditions for air. The paths inside the engine are modelled with multiple pipes, splits and orifices so that the real gas path in the engine is recreated. The model is found on the attached CD together with simulation setup for the different cases and the simulation results (License for GT-POWER is required to view this).

8.3. Calibration

The model has been used by Nabil Al Ryati for several load cases and therefore calibrated for these. In this study a fixed speed of 720 rpm will be used. The load is set to 80% of MCR corresponding to 945 KW. The model is built with a speed and load controller. These values are inputs and the model will seek the variables for temperatures pressures and mass flow through the engine for this input based on the engine model. Engine characteristics from test bed measurements for the same load and speed are provided in appendix 2. The simulation model provides much more detailed results throughout the whole engine. The corresponding engine parameters from the simulation model are listed in appendix 3. After some calibration the model worked well within an error of 2% for the measured parameters, which was a good correlation (Ryati 2010). The max cylinder pressure however is deviating by 5 bar or roughly 4%, which may be due to several reasons. Measuring cylinder pressure is not an easy task and errors can easily occur.

Exhaust temperatures are also outside the 2% range. The reason for this is mainly the difference in measured temperature at test bed and the simulated temperature. The simulation model is a non-predictive model with a fixed burn rate. This simulation model will be a relatively rough estimation of the combustion process.

8.4.Ambient conditions

Engines are normally tested and delivered with ISO standard ambient conditions as a reference for the engine performance. Most engines and especially engines used in marine applications normally operate with shifting ambient conditions both due to weather/season and location. The KRG-6 engine is an engine both used for marine and stationary applications. It is therefore interesting to investigate the effect of changes in ambient conditions to understand the altered performance. The focus is to simulate realistic ambient conditions but also look at what effect alteration of the four different parameters (air and sea temperature, humidity and pressure) does to engine performance.

8.4.1. Increased air temperature

Ambient temperature for marine diesel engines will normally not vary extremely because the temperature is strongly dependent on the sea temperature. The variation lies between arctic to tropic conditions. Normally temperatures of 0 to +45 degrees can be observed. If ambient temperature is known to be outside this window the engine must normally be re-matched using additional equipment such as charge air blow-of mechanism. The limits for normal operation (100% power available) for a standard ISO reference matched engine vary from manufacturer to manufacturer and engine type. The outside ambient temperature may differ from the engine room temperature measured next to the engine air intake. This temperature difference is highly dependent on the installation configuration in the engine room. Engine room ventilation can be decreased in cold climate, to increase the temperature.(MAN-B&W-Diesel-A/S)

To better understand the impact of different ambient air temperature The Bergen diesel KRG-6 engine will be simulated. The simulation is set up with the following 5 different ambient air conditions.

Case		1	2	3	4	5
Ambient air	K	275	285	295	305	315
Pressure	bar	1,022	1,022	1,022	1,022	1,022
Coolant temp	K	298	298	298	298	298
Humidity	%	30	30	30	30	30

Table 4 Changing ambient air temperature simulation setup

The KRG-6 engine is designed to deliver 100% power from 0 deg C to 45 deg C without modifications (Rolls-RoyceMarineAS 2001).

Increasing air temperature results in altered air density. The compressor will deliver less air (kg/s) for case 2-5 than for case 1. The temperature out of the compressor will rise accordingly. With increased temperature, the receiver pressure normally will decrease accordingly. Max cylinder pressure will increase with lower temperature and the max temperature during combustion will fall. As a result of the decreased energy in the exhaust, caused by lower mass flow through the engine, the turbine will deliver less power to the compressor.

37
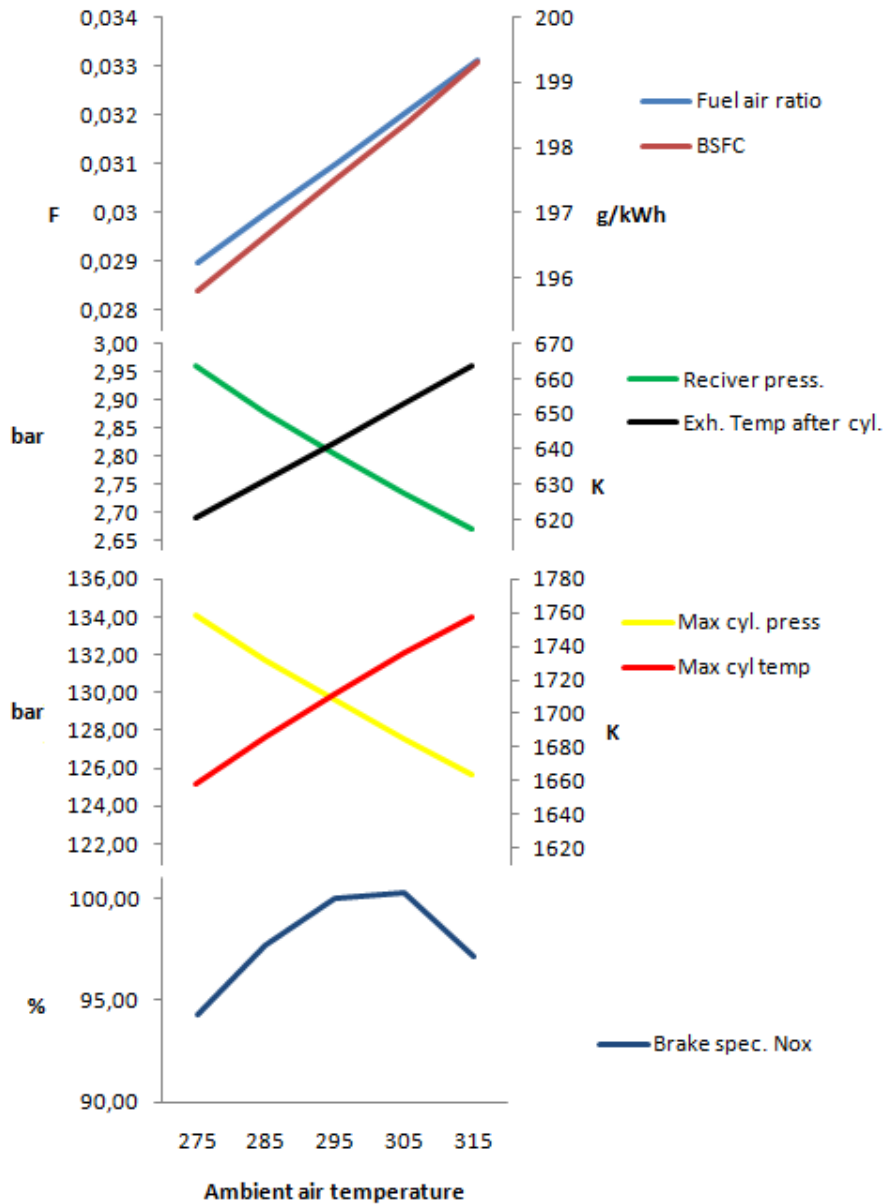
Figure 13 Simulation results from variation in ambient temperature

As the results show the trends stated earlier match the simulation trends shown in figure 13. SFC increase with 3 g/kWh for the measurements and the max cylinder temperature increase by 100 degrees. The NO_x emissions follow the increasing combustion temperature an increase. However the NO_x emission seems to flat out and decrease at high air temperature. As described earlier the factors affecting the NO_x emissions the most are the cylinder temperature, pressure. The cylinder pressure is reduced by 8 bars from case 1 to case 5 and represent a reduction of 6%. This reduction in pressure will contribute to a reduction in brake specific NO_x. The fuel/air ratio is becoming higher as the ambient temperature increases which means that less oxygen is available. This is also a contributor to the altered NO_x production presented in figure 13. Key parameters from the simulation are listed in appendix 4.

8.4.2. Increasing water temperature

The ambient water temperature determines the temperature of the cooling water used in the different systems on board. The engines internal cooling water system is linked to the sea cooling water system by a heat exchanger. It is important that the engine temperature lies within a certain range when the engine is running. Therefore the cooling water is controlled by a thermostat valve. The charge air can for some engines incorporate such systems, but often a fixed heat exchanger arrangement is used. This means that for such engines the changing sea water temperature will change the charge air temperature.

It is relatively easy to insert this to an engine performance computation. For the simpler models, which only involve combustion, the initial charge air temperature is altered. By implementing the charge air cooler to the model the sea water temperature at the heat exchanger is adjusted.

The KRG-6 GT-POWER model incorporates the charge air cooler. The temperature for the cooling water can therefore be adjusted and the effects evaluated.

Case		1	2	3	4
Ambient air	K	298	298	298	298
Pressure	bar	1,022	1,022	1,022	1,022
Coolant temp	K	273	283	293	303
Humidity	%	30	30	30	30

Table 5 Changing ambient water temperature simulation setup
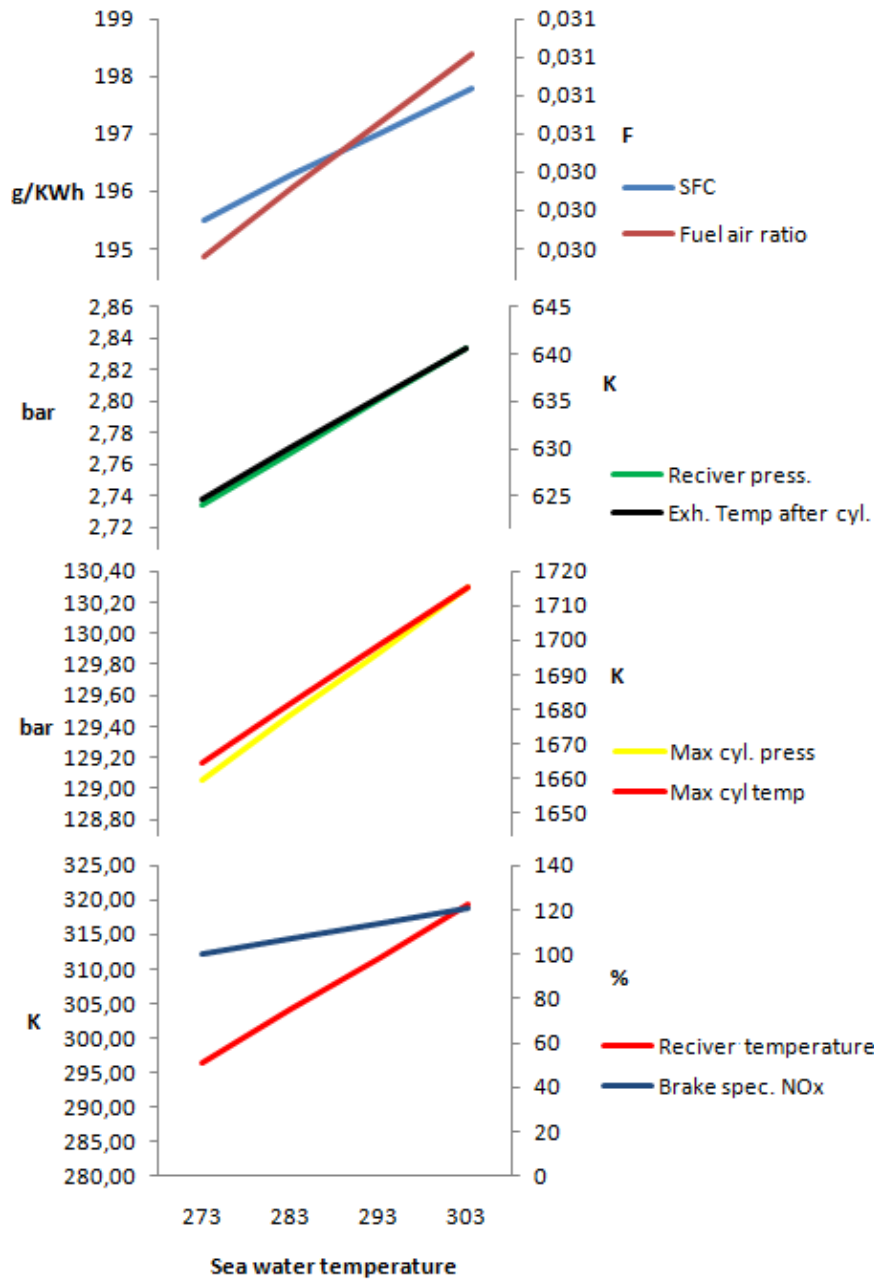
Figure 14 Simulation results from sea water temperature alteration

As expected, the resulting increase in the charge air temperature reduces the engine efficiency. This is mainly due to the reduced air density as the charge air temperature increases. The increased temperature is somewhat compensated for by the increased pressure in the charge air receiver. The reduction in performance is therefore not as severe as for increasing ambient air temperature. Normally the sea and the ambient air temperature are linked. Operating in tropical conditions may therefore require adjustments or limitations to prevent the engine from operating outside limits. Key parameters from the simulation are listed in appendix 5.

8.4.3. Increasing humidity

Humidity is a measure of the quantity of water in the air. The measure can be presented as relative or absolute humidity. ISO uses relative humidity of 30 % as standard reference condition. Relative humidity is the relationship between the amount of water vapour in air and the max amount of water vapour the air can contain when it is saturated. The definition is the relation between partial pressure for water vapour in a gas mix of air and water, and water saturation pressure for a given temperature. Relative humidity in percent is calculated as follows:

$$\emptyset_r = \frac{P_{H_2O}}{P_{H_2O}^*} * 100 \qquad (8.1)$$

$\emptyset_r$ -   Relative humidity for air

P_{H_2O} -   Partial pressure for water vapour in the gas

$P_{H_2O}^*$ -   Water vapour saturation point for the gas temperature

Case		1	2	3	4	5
Ambient air	K	294,5	294,5	294,5	294,5	294,5
Pressure	bar	1,022	1,022	1,022	1,022	1,022
Coolant temp	K	298	298	298	298	298
Humidity	%	30	40	50	60	70

Table 6 Changing ambient humidity simulation setup.

Humidity has impact on the engines performance and emission. The ISO reference condition states 30% relative humidity. Water vapour in the air reduces the density and oxygen and nitrogen molecules are replaced by water molecules. Five simulations of the KRG-6 engine have been performed. The humidity has been increased from 30 to 70 % at 294,5K air temperature. Impacts on the engine's performance have been evaluated. Key parameters from the simulation are listed in appendix 6. Figure 15 shows how some selected key parameters vary in the different cases.
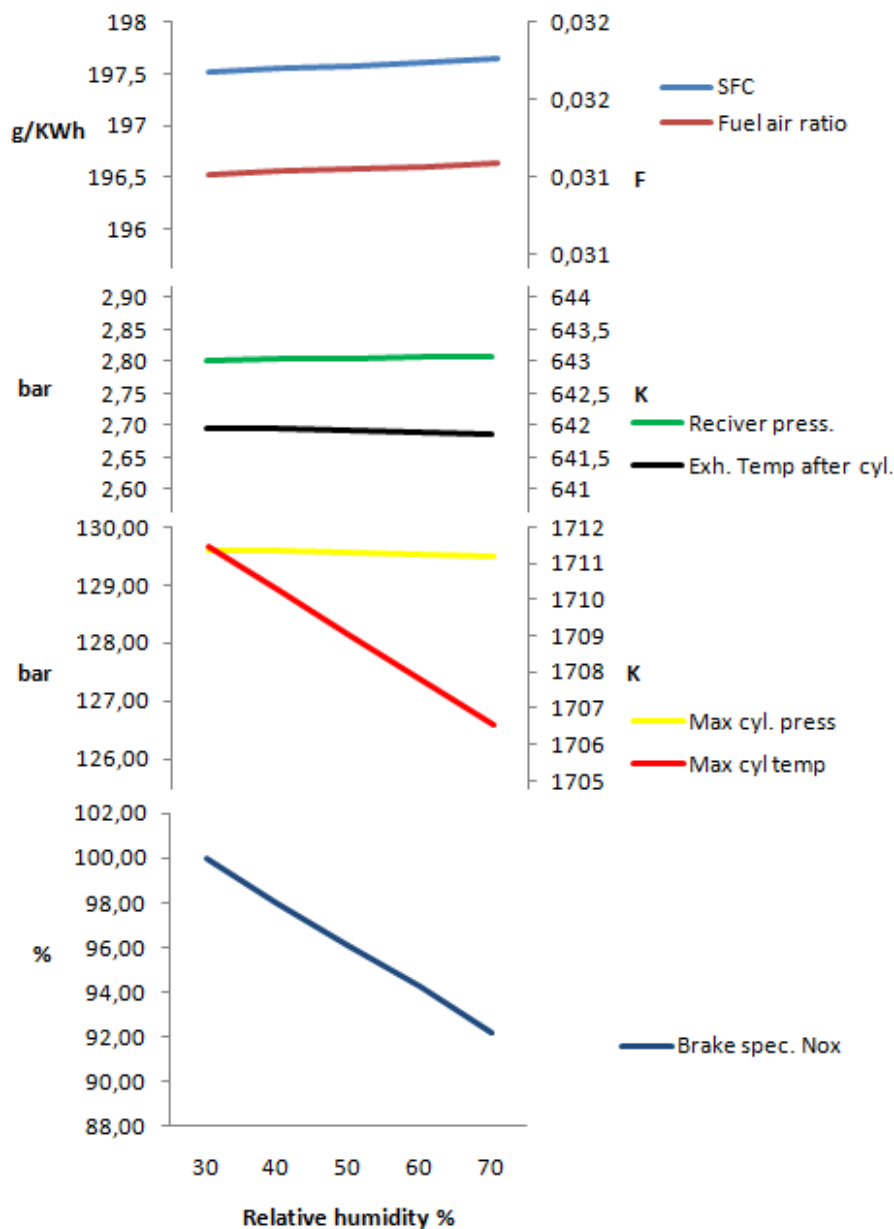
Figure 15 Simulation results from increased ambient humidity

As can be seen from the results, the humidity does not have a major impact on the performance. The increase in SFC is approximately 0,25 g/kWh which is not much. The NO_x emission is reduced by approximately 10 %. This is due to the reduced combustion temperature. The temperature is reduced because of the increased specific heat capacity of the air in the cylinder. Increasing humidity or generally introducing water in the combustion either directly or by emulsion is a well known method to reduce the NO_x emission without significantly reducing the engines efficiency.

8.4.4. Decreasing ambient pressure

Ambient pressure is constantly shifting according to the weather conditions. Decreasing ambient pressure reduces the air density and alters therefore the compressor work, pressure throughout the engine and fuel air ratio. The TC speed will increase as a result of the lower density (less work per W/m³ air) and the relatively more power from available the turbine. A reduction in airflow through the engine directly is linked to the reduced receiver pressure as a result.

Simulations for reduced ambient pressure have been performed. Five different simulations have been set up, starting at an ambient pressure at 1,022 bar and reducing it by 0,050 bar for each case. The ambient condition in the first case is the same as for the shop trials for the engine.

Case		1	2	3	4	5
Ambient air	K	294,5	294,5	294,5	294,5	294,5
Pressure	bar	1,022	0,972	0,922	0,872	0,822
Coolant temp	K	298	298	298	298	298
Humidity	%	30	30	30	30	30

Table 7 Changing ambient pressure simulation setup
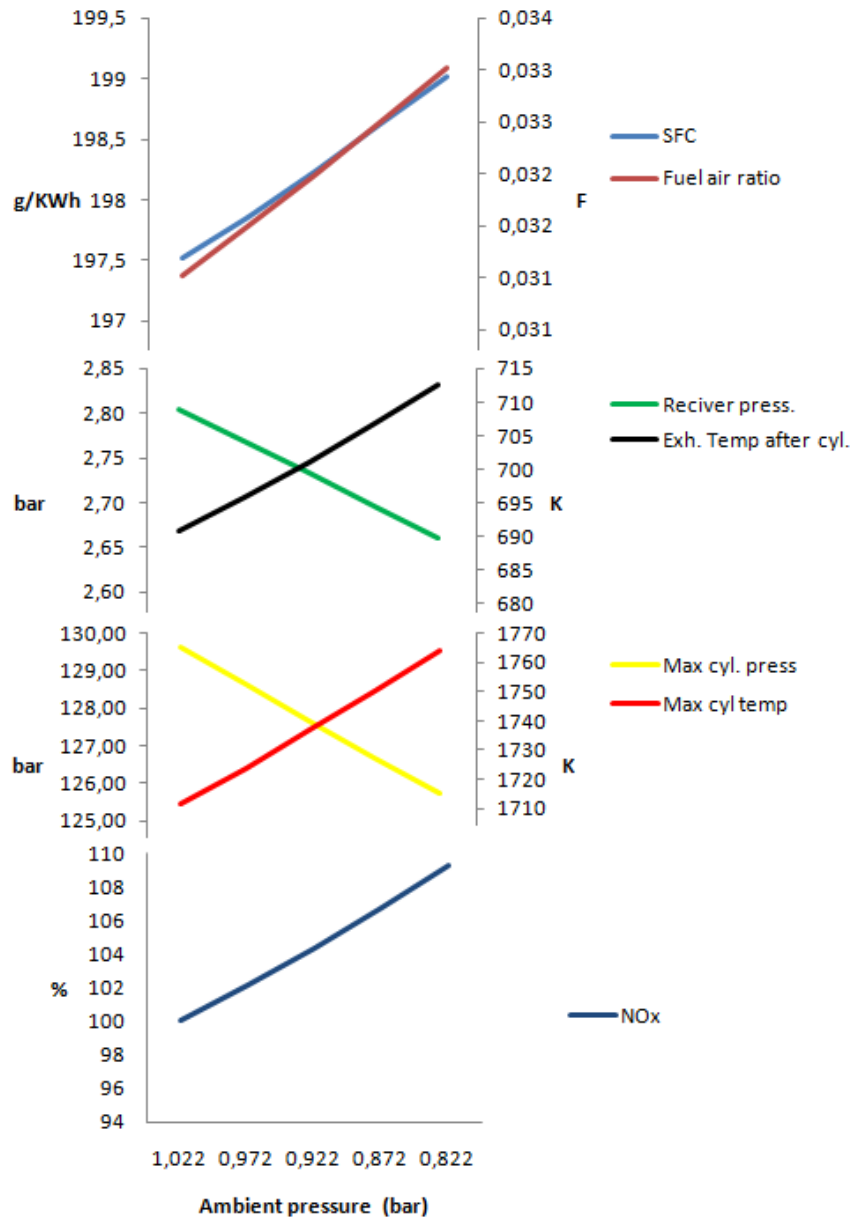
Figure 16 Simulation results from variation in ambient pressure

As expected the simulations show reduction in performance. The SFC is increased as a result of the lowered air flow into the engine. Consequently the cylinder pressure is reduced. And the max temperature is increased. NO_x emissions are rising by 10% from case 1 to 5 due to the increased temperature. As the cylinder pressure is not reduced more than 4 bar the effect seen for increased ambient temperature regarding NO_x is not present here. Key parameters from the simulation are listed in appendix 7.

8.4.5. Comparison with non reference condition calculations

A non reference calculation based on the ISO 3046 standard was performed regarding increase of fuel consumption as a result of increased ambient temperature and humidity stated in table 3. The same ambient conditions have been simulated in GT-power for the KRG-6 engine. The results from the simulation indicate an increase in SFC to 198g/kWh. The ISO correction estimates the SFC to be 197,5 g/kWh. The difference is 0,5 g/kWh.

It is interesting to see how the trend for both ISO estimations and simulations deviate for other temperatures. Several ambient temperatures has been simulated and estimated. The result can be seen in figure 17. Standard ambient reference condition has been simulated and used as reference point. Details are presented in appendix 19.
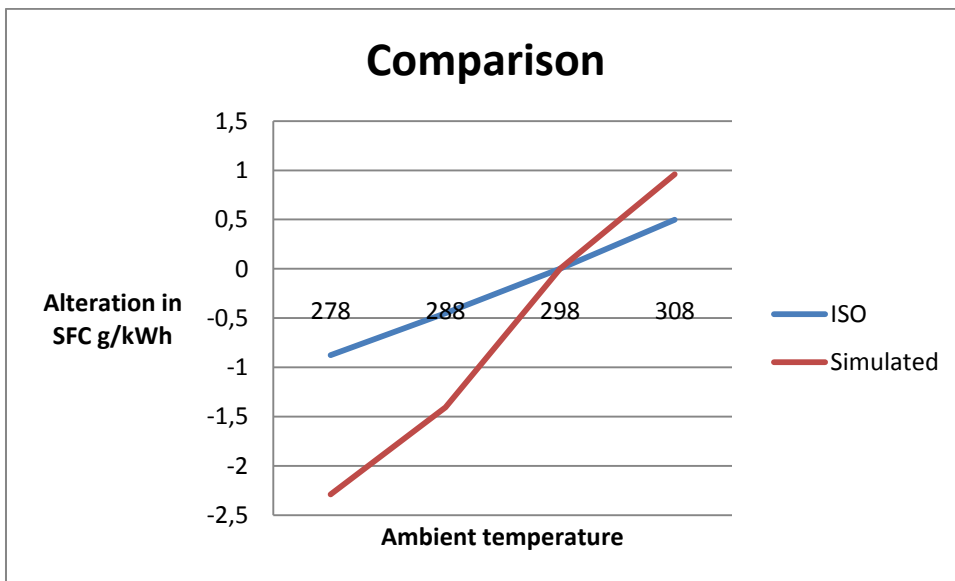
Figure 17 Comparison between ISO correction and Simulations in GT power

The ISO correction results in a linear increase in SFC as the temperature rises. This was expected since the ISO correction is based on the airflow through the engine. The simulation indicates a steeper increase in fuel consumption as the temperature increases. The simulation is more likely to be closer to the actual SFC based on the fact that the simulation model includes additional factors such as heat transfer in the cylinder and altered flow in turbine and flow pipes. Based on the comparison it can be concluded that the ISO correction is a conservative estimate of the alteration in SFC due to increasing ambient temperature for this engine. Comparison with the real engine performance for the different ambient conditions has not been possible because those data has not been available.

8.5. Conclusion ambient conditions

As identified all ambient conditions have an impact on the engine performance if they change, some more significantly than others. It is obvious that it is the air temperature and pressure that affects the performance the most. In extreme situations measures such as reducing power or implementation of additional equipment might be necessary to avoid operation outside limitations. The NO_x results from the simulations are not correct. There reason is that test bed data were incorrect and could therefore not be used to calibrate the model. However the trend line that the results give will be closely matching the real engines alteration in brake specific NO_x. ISO 3046 and 15550 is developed to recalculate amongst other power and fuel consumption for an engine not operating at ISO standard conditions. It has been shown that the results from simulations and estimation from ISO correction is closely matching. The ISO correction seems be more optimistic in the region above ISO standard conditions, and the other way around for temperatures beneath ISO standard condition. Since ISO correction is estimations for all types of engine it is likely to assume that the simulation results are closer to real observations.

8.6. Fault conditions

Diesel engines will over time develop fault conditions either as a result of normal wear or because of incorrect use such as overloading. Such faults can be introduced to an engine simulation by e.g. altering the efficiency for the turbine. Four fault conditions have been investigated. The following subchapters describe how these fault conditions are introduced to a simulation program. Simulations with fault conditions are performed and the results are presented and discussed relative to the new condition.

8.6.1. Compressor condition

The compressor can gain fouling or be exposed to wear that alters the geometry in the compressor. This will cause reduction in compressor efficiency as a result of normal wear and or by inefficient air filter which allows particles to flow through the filter.

A reduction in compressor efficiency will result in reduced airflow to the cylinder. The reduced airflow will reduce the air excess in the combustion and further decrease the max cylinder pressure, increase the exhaust temperature, increase fuel-air equivalence ratio and consequently increase the production of NO_x (Hountalas 2000).

The compressor theoretical isentropic efficiency can be determined as follow:

$$\eta_{compressor} = \frac{T_1 \left(\frac{P_2}{P_1}\right)^{\frac{\kappa_{Air}-1}{\kappa_{Air}}}}{T_2 - T_1} \tag{8.2}$$

A reduction in the efficiency, assuming that the engine operates on a fixed load and speed, can be detected as alteration of either pressure or temperature (or both) after the compressor. However it can be difficult to detect this in a running engine as a fault condition in other components can give impact to other "healthy" components. Ambient condition will also give impact on these readings. It is therefore beneficial to model this and get an indication to how this fault condition affects the engine performance.

Alteration in the efficiency can be calculated as follow(Rasmussen 2003):

$$Condition\ Parameter$$

$$= \frac{Reference\ parameter - Operation\ parameter}{Reference\ parameter} \tag{8.3}$$

$$\Delta\eta_{compressor} = \frac{\eta_{comp.ref.} - \eta_{comp.op.}}{\eta_{comp.ref.}} \tag{8.4}$$

The reference parameter is obtained from measurements when the engine is in new condition. A reduction in air receiver pressure will lead to reduction of power for the engine as especially the exhaust temperature will exceed the max operating limit.(Hatlevold 2009)

1 Turbine wheel with shaft
2 Compressor wheel
3 Bearing casing
4 Bearing sleeve
5 Gas admission casing
6 Nozzle ring
7 Exhaust gas diffuser
8 Gas outlet casing
9 Compressor casing
10 Air diffuser
11 Silencer
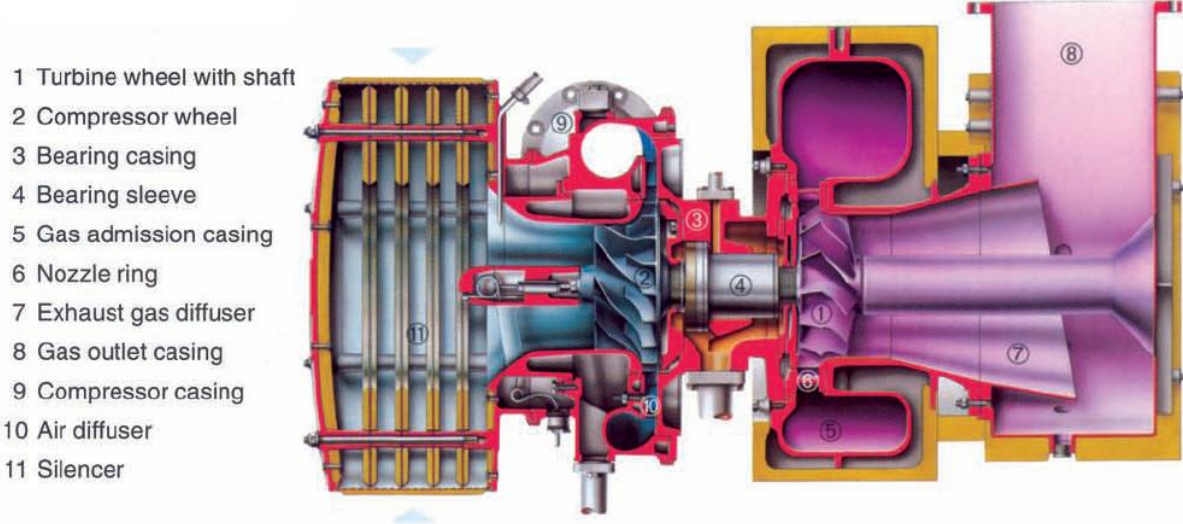
Figure 18 Cross section of MAN NR/S type turbocharger (MAN-Diesel)

To simulate reduced compressor condition the efficiency multiplier in the compressor template is varied from 1 to 0.8 in 5 different cases.

Reduced compressor efficiency results in reduced charge air pressure. As stated earlier the reduction of charge air pressure will result in reduced compression pressure and max pressure in the cylinder. This reduction will influence the engines efficiency negatively (Stapersma 2009).In order to keep the MEP constant the combustion must last relatively longer than for normal condition. The expansion process is to some extent deteriorated. The temperature in the cylinder is closely connected to the pressure but since the fuel-air ratio is increased and more fuel is burned, the temperature will increase as the compressor condition is worsened. The increased temperature will contribute to a higher heat transfer to the walls in the cylinder resulting in a larger heat loss. The effects described above are al responsible for reducing efficiency of the engine and consequently increasing the SFC. NO_x formation is increased drastic as a result of the increasing combustion temperature and relatively more fuel injected to maintain the mean effective pressure corresponding to the speed and

power setting. The effects can be seen in figure 19 for some selected parameters. A more detailed list is presented in appendix 8.
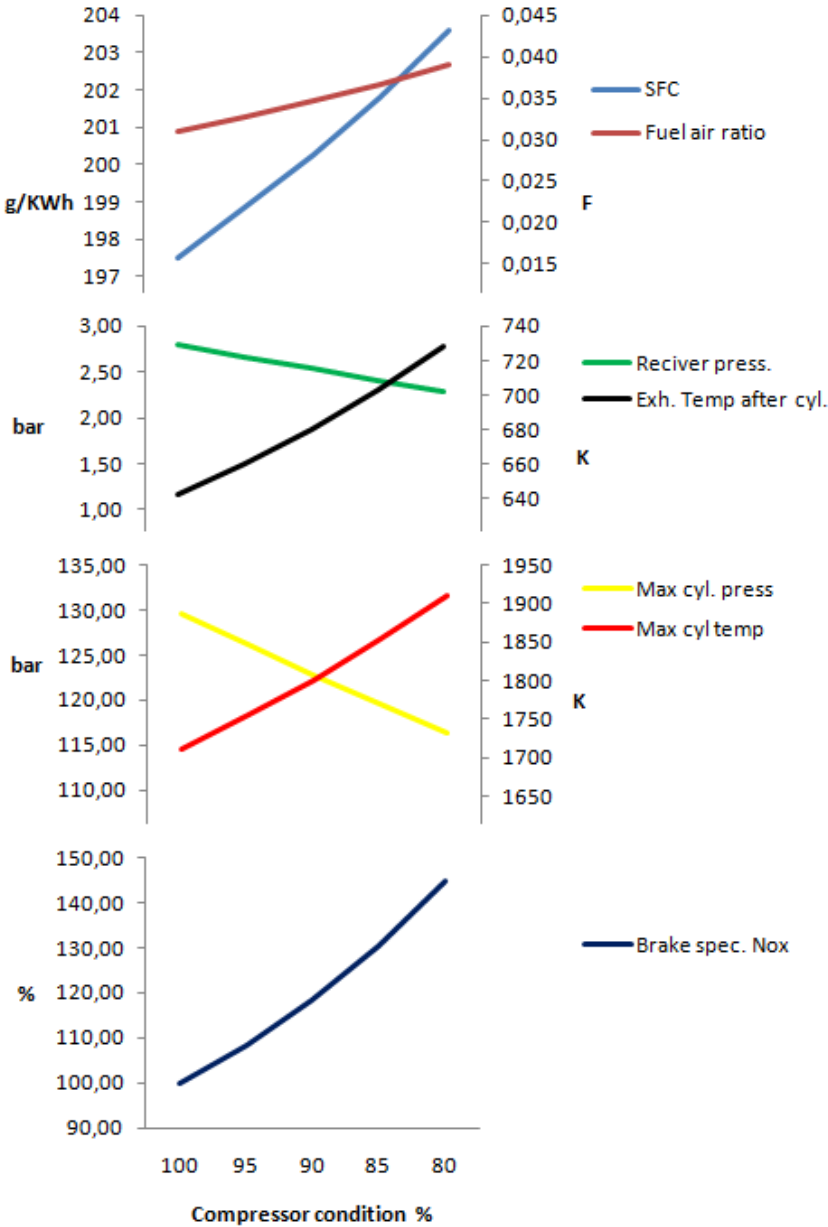
Figure 19 Simulation results from reduced compressor efficiency

As can be seen from figure 19 the reduced compressor efficiency will rapidly result in reduced performance for the engine. To avoid this fault condition the air filter must be replaced or cleaned regularly and the compressor must be cleaned.

8.6.2. Turbine condition

The turbine is situated in the exhaust flow from the engine. The exhaust gas from a diesel engine is polluted with contents of ash, unburned hydrocarbons and particles in addition to the pollutants in gas phase. These pollutants in combination with high temperature will over time foul and wear the turbine so that the aerodynamics of the turbine geometry changes. This change will lead to a reduction in the turbine efficiency and further reduce the power delivered to the compressor. Furthermore this will result in a reduction in receiver pressure and reduced airflow through the engine. The combustion temperature and exhaust temperatures will rise.

The necessary mitigation to prevent this is to regularly clean, overhaul or replace the turbine when necessary. The condition can be monitored by evaluating the pressure drop over the turbine and temperature drop over turbine and thereby calculate the isentropic efficiency.

$$\eta_{isen.K} = \frac{T_1 - T_2}{T_1 - \left(\frac{P_2}{P_1}\right)^{\frac{\kappa_E - 1}{\kappa_E}}}$$ (8.5)

It is important that the measurements taken in order to calculate this efficiency are done during similar conditions i.e. speed, load and ambient conditions.

The condition has been introduced to the GT-power model of the KRG-6 engine by reducing the efficiency multiplier in the turbine template from 1 to 0,8.
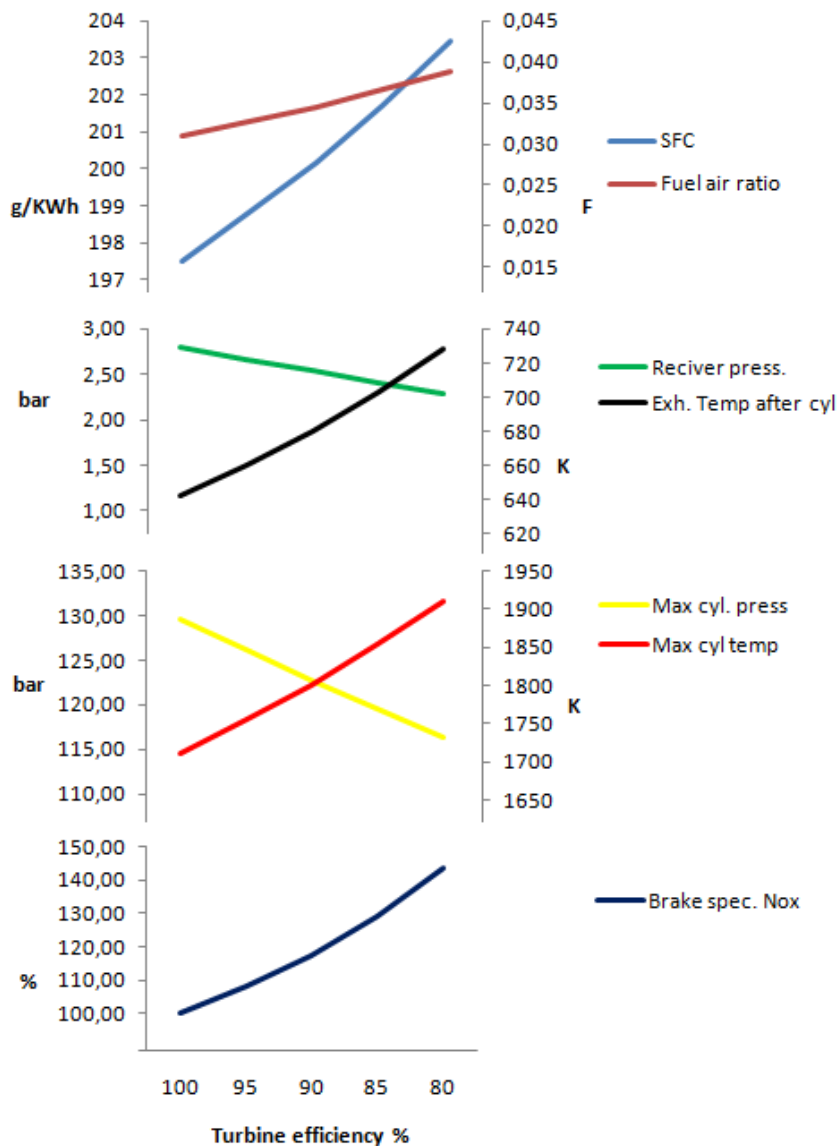
Figure 20 Simulation results from reduced turbine efficiency

This condition has more or less the same influence to the engines performance as the reduced compressor efficiency. The difference and way to identify one from another is to look at the temperature drop (delta T) over the charge air cooler. For reduced turbine condition this temperature drop is small compared to reduced compressor condition where the temperature drop stays more or less constant. The reason for this is that the efficiency for the compressor is good in the case of decreased turbine efficiency, resulting in a good compression and a "normal" temperature rise relative to the pressure rise. When the compressor condition is reduced the temperature after compressor does not drop more than a few degrees when the condition is reduced by 20 % even though the pressure is significantly reduced (Hountalas 2000).
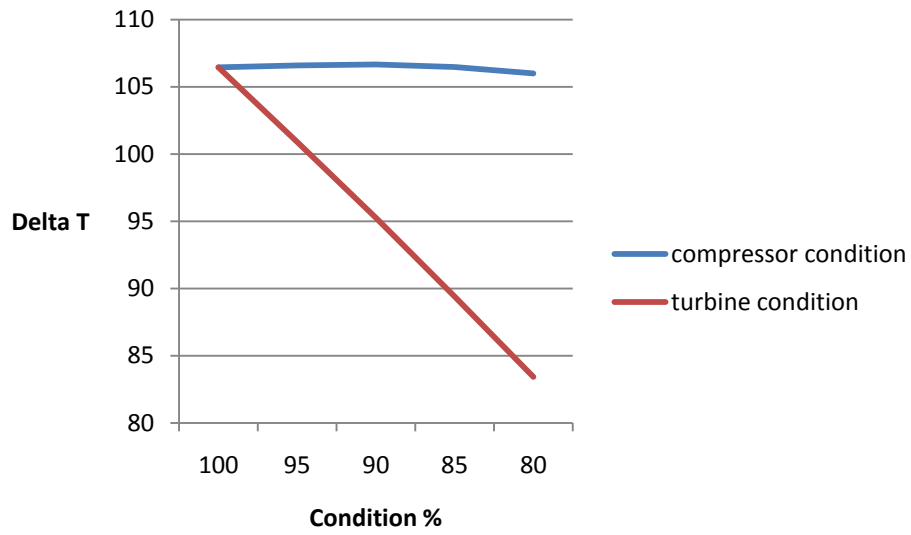
Figure 21 Temperature difference over charge air cooler for reduced turbine and compressor condition.

8.6.3. Injection timing

This fault condition is a result of incorrect timing between the engines fuel cam shaft and crank shaft, wear to the fuel pump rollers or wear of the fuel cam shaft. (Hountalas 2000)

A slight change in injection timing will result in alterations to the performance for a diesel engine. An increase of injection timing before TDC usually results in an increase in efficiency, maximum combustion pressure and temperature (to a certain point). The exhaust temperature will decrease because of the improved expansion process. This effect will also result in a reduced receiver pressure due to less energy in the exhaust. This reduces the mass flow rate through the engine. Decreasing the injection timing towards the TDC will cause the opposite effects.

NO_x emissions are as described strongly dependent on the max temperature and pressure during the combustion. As the temperature increase with advancing injection timing the NO_x emissions will increase.

NO_x emission is taxed and measures to reduce these emissions are developed and implemented. One of the primary methods of reducing NO_x emissions is to retard the injection timing. By doing this, NO_x emissions can be reduced significantly. The penalty of course is an increase in SFC.

For the Bergen diesel KRG-6 engine nine different timing settings have been simulated; from 8, 5 to 15, 5 degrees before TDC with one degree step. The original setting is injection timing corresponding to 12, 5 degrees before TDC.
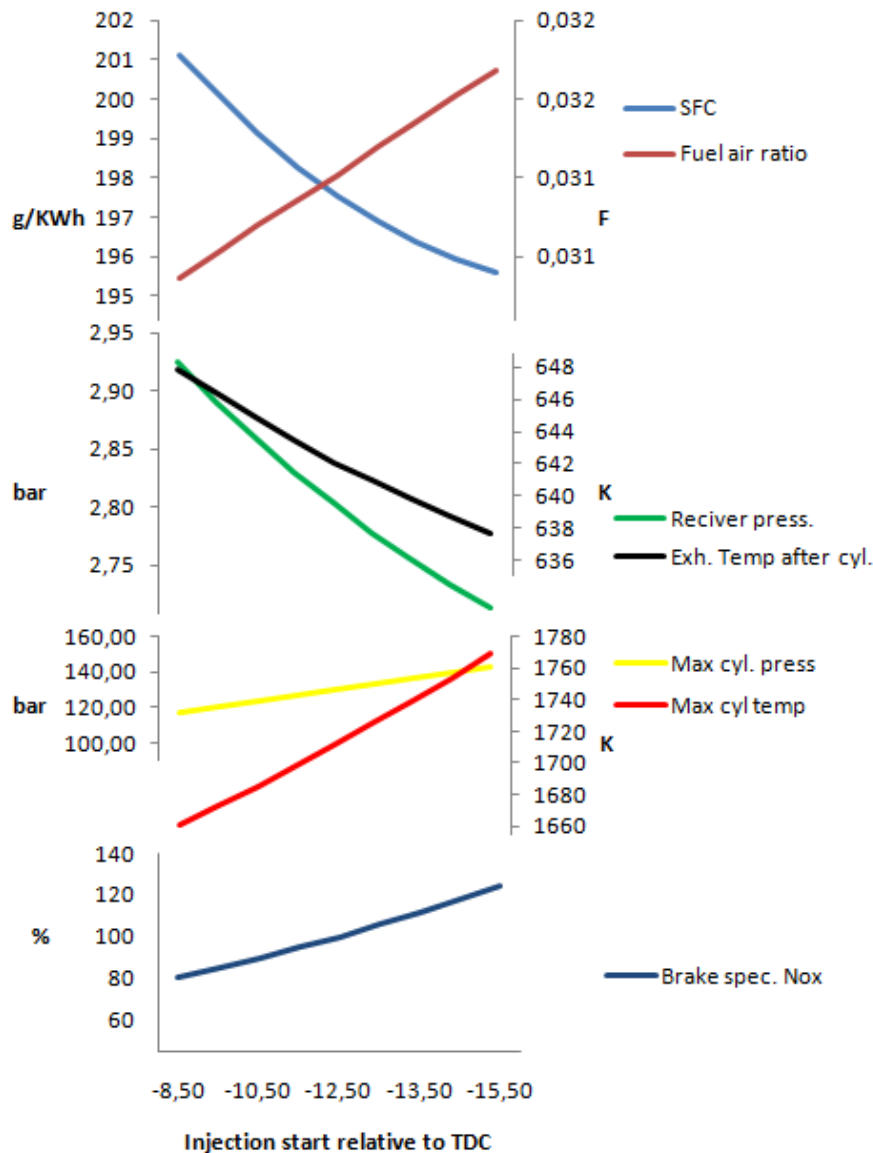
Figure 22 Simulation results from ignition variation

As can be seen in figure 22 the results from the simulation are complying with the previous mentioned effects of varying ignition timing. Minor injection timing faults will not lead to threatening conditions for the engine but will result in increased or decreased SFC depending on which direction the timing is moved. Max cylinder pressure will increase rapidly as the timing is increased and may result in pressures above allowed limits. The max pressure is affected by the relatively larger portion of fuel burning in the premixed faze. The reason for the relatively larger portion burning in the premixed faze is that the ignition delay will increase due to the lower temperature and pressure at the start of injection. Also the TDC is occurring later in the combustion process. The temperature is dependent on the pressure in the combustion chamber, but also of the fuel/air ratio which is increasing when increasing injection timing. These two conditions drive the combustion temperature up. Both Wartsila and MAN B&W have systems for variable injection timing (VIT) for some of their engine types. The system was introduced to increase the efficiency at part load. The timing would also be possible to adjust to take into account poor fuel quality. However, adjusting the timing should not be done to compensate for wear of the engine (N.E Chell 1999).

8.6.4. Cooler efficiency

Engines are turbocharged to increase the amount of air going in to the cylinder; more fuel can then be burned. As the charge air is compressed it becomes hotter and density drops relative to cool air at the same pressure. The charge air cooler is installed to reduce the temperature and increase the density of the charge air. A second benefit is that the cooled air reduces the thermal load of the engine. Charge air coolers are usually tube type coolers.(N.E Chell 1999)

The heat exchange area in the cooler will over time be fouled and the heat exchanging efficiency will decrease. The decreased efficiency will lead to higher scavenge air temperature and hence a lower air density. The reduction in density is not large since the air receiver pressure will be relatively larger. As the air side is fouled the pressure drop across the cooler will increase. The pressure drop will not be evaluated here.

An alternative to clean or replace the cooler is if possible to reduce the cooling fluid temperature or increase the flow of cooling fluid. If such measures are available they will however only be a postponement of the maintenance work that needs to be done.

Assuming a counter flow heat exchanger is used, the efficiency of the heat changer can be determined by:

$$\eta = \frac{T_3 - T_4}{T_3 - T_1} \tag{8.6}$$

T_1 Water inlet temperature
T_3 Air inlet temperature
T_4 Air outlet temperature

If the water inlet temperature and the air inlet temperature are kept constant we can determine the new air outlet temperature based on a reduction in the heat exchanger effectiveness. (Eilif Pedersen 2008)

$$T_4 = T_3 - \eta * (T_3 - T_1) \tag{8.7}$$

Reduction in heat exchanger effectiveness is mainly caused by reduced heat exchange area and an increasing heat conduction coefficient both as a result of pollution (Hountalas 2000). To handle this problem the cooler has to be cleaned or replace even though adjustments are done to temporary reduce the effect.

The Bergen Diesel KRG-6 engine has a two stage charge air cooler. Simulations have been performed for this engine at 720rpm and 80% load. The second stage air cooler efficiency was dropped from 100% to 60% of. The effect on the engine is presented in figure 23 below and in more detail in appendix 12.
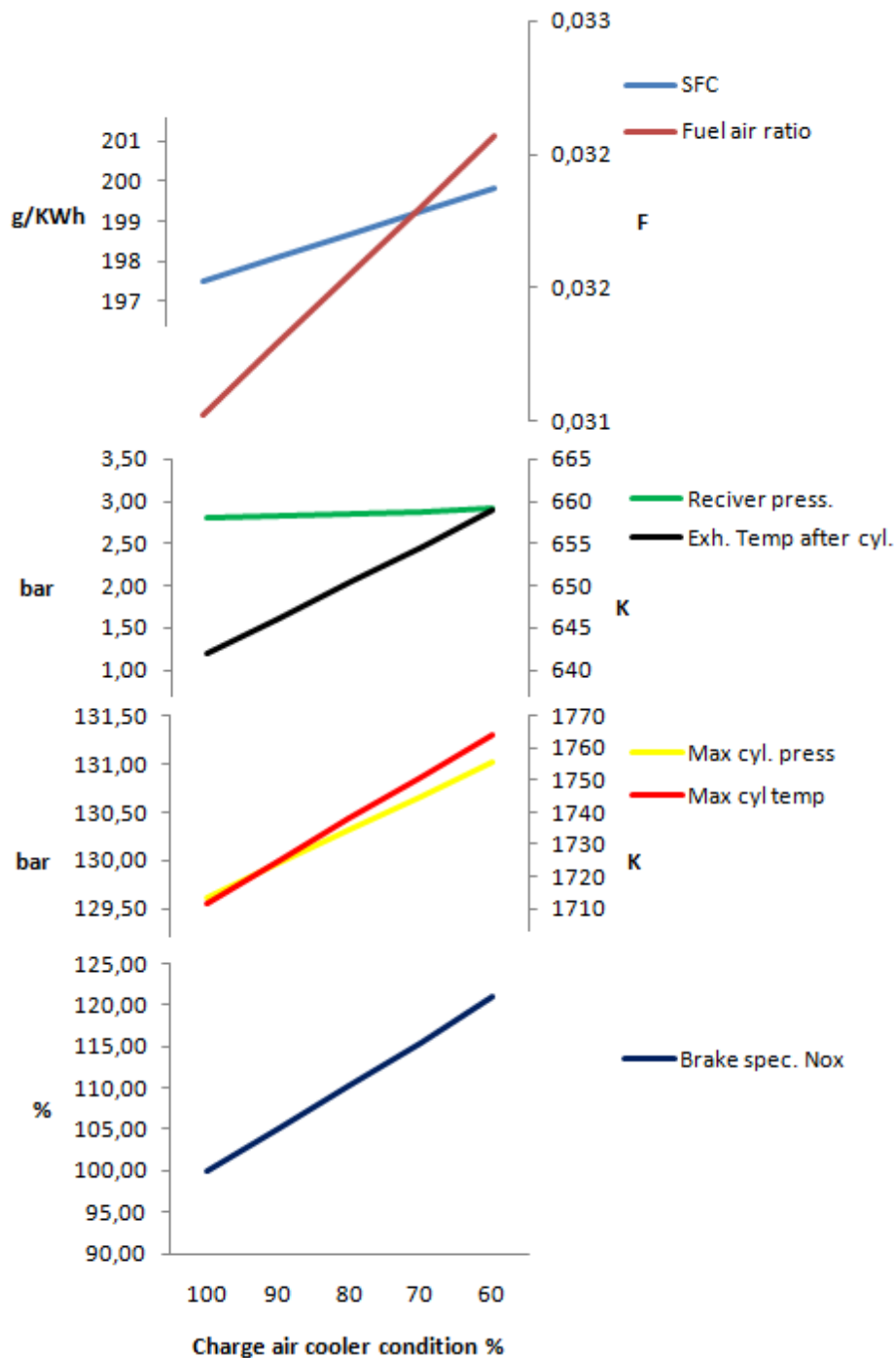
Figure 23 Simulation results; declining second stage charge air cooler efficiency

As can be seen from the simulation results, the second stage cooler efficiency must be significantly reduced to impose considerable changes to the engine performance. With the air cooler efficiency reduced 40% the increase in SFC is just above 2 g/kWh. The parameter that is most affected is the exhaust and cylinder temperature. The increased temperature is a result of the lower air density and hence the lowered air fuel ratio but also the lack of the cooling effect from the cool charge air.

It is interesting to investigate if changes made on the cooling water side of the charge air cooler can reduce the effect of a fouled charge air cooler. By setting up a new simulation based on the 60%

cooler condition and reduced cooling water temperature, the effect of doing such measures can be quantified. The results can be seen below:

Cooler efficiency	%	60	60	60
Cooling water temp	K	278	288	298
Performance with reduced cooling water				
SFC	g/KWh	198,9	199,4	199,8
Max pressure	bar	130,5	130,8	131,0
max temperature	K	1744	1754	1764
Charge air				
Temperature	C	330	335	340
Pressure	bar	2,87	2,89	2,91

Table 8 Reduced cooler efficiency with reduced cooling water temperature

This simulation is based on reducing the second stage cooling water temperature. A reduction of 20 deg. cooling water temperature will reduce the SFC by approximately 1 g/kWh. The temperature will decrease by 10 deg. This kind of adjustment is not commonly available and a reduction of 20 degrees is not feasible to achieve in most operating areas because the temperature of the sea water is fixed.

A more realistic way to handle such a problem temporarily is to increase the flow of cooling water. It is not possible to manipulate this in the GT-POWER model of the Bergen Diesel engine. Looking at the energy balance this becomes clear. If the $\dot{m}_{C.W}$ is increased and all other parameters are kept constant, the $T_{out,water}$ will drop.

$$d\dot{Q}_{Air} = C_{p,air} * \dot{m}_{Air} * (T_{in} - T_{out})$$
$$d\dot{Q}_{C.Water} = C_{v,c.water} * \dot{m}_{C.W} * (T_{out} - T_{in})$$
$$d\dot{Q}_{Air} = d\dot{Q}_{C.Water}$$

(8.6)

This measure will not be further investigated here.

8.7. Conclusion fault conditions

The fault conditions examined in this thesis are typical fault conditions that can arise during a diesel engines' lifetime. The faults are all corrected by performing maintenance, either preventive or scheduled. If the fault condition is allowed to escalate the engine might operate without limits or limitations to power or speed will be necessary. Fuel consumption will increase for all fault conditions (except advanced injection timing). The impact to the fuel consumption is of course different from case to case, but generally it will lead to increased operation cost. The same conclusion regarding NO_x emission prediction from GT-POWER can be made her. TC condition is the condition that will affect the engines performance most rapidly of the four analysed conditions. Several degrees of incorrect injection timing will also impose a significant alteration to the performance, but this is not something that normally occurs due to normal wear. A miss alignment of the fuel cam shaft would have to be done to gain large deviations.

9. Case; Simulation of a B&W &L67GFCA diesel engine

9.1. Case background

Kristian Gerard Jebsen shipping company (KGJS) technical support division is situated in Bergen. The division is currently investigation how engine and hull monitoring reports can be used to better optimize the performance and earlier detect changing conditions to KPI for the ships in their fleet. The suggested KPI from KGJS are:

- Deviations and absolute values of P_{max}, P_{comp} and P_{mi}
- Exhaust temperature
- TC rpm
- Scavenge air pressure
- SFC
- Lube oil consumption
- Cylinder oil consumption
- Running hours, auxiliary engines
- Fouling condition

These KPI's can be collected from the current engine reports received by the division. The focus in this thesis will be the performance of the main engine excluding cylinder and lube oil consumption.

One of the older ships managed by the KGJS (the M/S Siskin Arrow), has reported low scavenge air pressure on the main engine. The technical division at KGJS is trying to establish what impact this reduction will inflict on the SFC. The condition on M/S Siskin Arrow is a condition that has been developing for some time, and it is believed that if a proper engine monitoring system had been in use this condition would have been detected earlier. A proper action could then have been taken earlier in the condition development. The technical division is interested to understand the correlation between reduced scavenge air pressure and increased SFC. As an estimate the factory has stated that a decrease of 0,1 bar scavenge pressure will result in an increase of 1 g/kWh SFC.

By use of a simple simulation program this correlation will be modelled to see if it is an accurate figure. The program that will be used is the POWER-CYCLE developed at Marin technology, NTNU.

9.2. Engine data

The engine is a 6 cylinder, 2 stroke engine manufactured in 1983. Some of the engines data and average running parameters are listed in table 9, for all six cylinders. The total test bed data are listed in appendix 13. The compression pressure obtained from this chart is relatively high for such an engine and corresponds to a compression far too high for this engine. It is therefore assumed that this data is incorrect. It has been a problem to gather a set of complete data necessary to perform the analysis. Therefore some assumptions and qualified derivation have been made regarding compression ratio and cylinder volume. In addition some qualified assumptions have been made for the inputs to the simulation program. These will be discussed in the chapter concerning the actual simulation.

Bore	760	mm
Stroke	1700	mm
Comp. ratio	12.12	-
Power	7269	KW, 100% @117 rpm
Scavenge air pressure 100%MCR	1,93	Bar
Max pressure	90	Bar
P_{comp}	57	bar
Data retrieved from test bed results at 123rpm/100%		
$T_{exhaust}$ after cylinder	358	C
Temp scavenge air	41	C
Fuel consumption	192,11	g/kwh

Table 9 MAN B&W 6L67GFCA engine data from test bed at 117 and 123rpm at 100% load.(Not the engine onboard MS Siskin Arrow)

9.3.Power cycle analysis

Power cycle is a FORTRAN based thermo dynamical analysis program dedicated to the four stroke diesel engine. The program is developed by Professor Harald Valland at Marin technology, NTNU. The program is designed to simulate four stroke diesel engines but by doing some minor adjustments and simplifications we can adopt it to give meaningful results for 2-stroke analysis. As the POWER-CYCLE program is a relatively low tech program compared to the previously used GT-power program, the results will not be as accurate but trends in question can be determined. The reason for using POWER-CYCLE instead of using the GT-POWER program is that it requires less work to use and provides fast and good results and the model requires much less input data than GT-POWER models.

9.3.1. Method of computation

Computation of thermodynamic properties for the working media is the basic routine in the program. The properties for the different states are calculated based on the input data for the fuel and the oxidant composition. The composition of the products in terms of mole fractions is computed using either fuel-air equivalent ratio (F), pressure or amount of fuel burned to determine the end state properties. The thermodynamic properties are then computed based on the mole fraction and data for the individual species. Further a set of reverse routines using the same p, T and F are implemented in the program. These routines are used for computation of simple cycles including combustion. During compression, expansion and heat interaction the composition does not change and the computation of end stat properties is then only a function of pressure and temperature.

The process analysis is focusing on the work and alteration in properties from a given initial state to an end state. Combustion on the other hand involve reactants and products and lead to a new working media composition. Fuel is defined by the composition $C_nH_mO_lN_k$ and the energy related to the fuel; LHV. End state properties after constant volume and constant pressure combustion can further be determined. End state calculation for constant volume combustion requires input for either p, F or fraction of burned fuel to be determined. End state for constant pressure can be

59

defined by F or it can be specified as a free variable so that a predefined mean indicated pressure can be found. The program returns state conditions for the 9 stages of the engine cycle. The different stages are illustrated and described in chapter 2.2 (Valland 2008).

9.3.2. Estimating compression ratio

KGJS has provided engine data and shop trials for this type of engine. These data are provided in appendix 13. Not all the data required were provided such as compression ratio (CR). Compression ratio is a function of mainly three variables; the cylinder geometry (bore and stroke), compression volume and volume at TDC. Only data for the cylinder geometry has been available, so qualified assumptions have been made to retrieve the two others.

$$CR_{effective} = \frac{V_c + V_{TDC}}{V_{TDC}} \qquad (9.1)$$

V_c is the compression volume when the cylinder is sealed off and exhaust and inlet ports are closed. For this engine it is assumed to be 94% of the stroke volume. The top dead centre volume is assumed to be 8,45% of the stroke volume, leading to an effective compression ratio of 12.12 which is a typical figure for this type of engine (Valland 2010). These assumptions will most certainly lead to an error in the results when comparing to the real engine, but since this is used for all simulations the trend that occurs from these will give meaningful result.

9.3.3. Power cycle simulation input

The purpose for the simulation is to investigate how reduced charge air pressure affects the overall performance with focus on the specific fuel consumption. 5 simulations have been performed with different charge air pressure from 1,93 to 1,53 bar absolute pressure. The inputs for the program can be seen in table 10. Each input will be further discussed.

Bore	0,67	m
Stroke	1,70	m
Compression ratio	12,12	-
Charge air	1,93	bar (initial)
Charge air temperature	314,00	K
F1	0,00	-
LHV	41,50	MJ/kg
Crank arm ratio	0,41	-
Pressure difference Inlet to Exh	0,19	bar
pressure drop across valves	0,00	bar
Volume at start of compression	0,61	M3
Isentropic compression	yes	-
Heat loss	10,00	%
Pressure difference combustion at constant volume	35,00	bar
F4	0,6	-
Isentropic expansion	yes	-
Target Mean indicated pressure	11	bar
Free variable	F4	-

Table 10 Inputs to the Power-cycle simulation program

Compression ratio

The effective compression ratio was found by means of some qualified assumptions. It should be noted that the effective compression ratio is different from the nominal compression ratio. The nominal compression ration utilizes the bottom dead centre volume instead of the compression volume. Using the nominal compression ratio will lead to a higher pressure after compression.

Charge air pressure

This parameter is the one in question in this case. The initial 1,93 bar is taken from the test bed results in appendix 13. This test bed measurement may have some divagations from the actual engine onboard the MS Siskin Arrow. This parameter is used as a start point for the simulations. The pressure corresponds to a higher revolution than the Siskin Arrow engine is designed for but is a good start point for the simulation. The SFC from the simulation is based on a revolution of 107rpm. The charge air pressure for this load and speed condition might be unrealistically high, but since data for the new condition regarding this pressure is not available this is what initially will be used.

Charge air temperature

The temperature is the same for all simulations and is retrieved from the same test bed results in appendix 13. The temperature will normally differ with the charge air pressure if not a thermostat controlled arrangement is incorporated or internally cooling with jacket cooling water is used. For simplicity and lack of data a fixed temperature of 4 °C or 314°K is used for all simulations. A lower air temperature will increase the air density and thereby slightly reduce the effect of reduced charge air pressure. Other effects such as increased ignition delay, caused by cooler air in the cylinder can in a certain degree affect the combustion. This effect cannot be simulated in the POWER-CYCLE program and will therefore not be addressed in this simulation.

Fuel-air ratio F1

It is assumed that the air in the cylinder is fresh air. The air composition is set to be the default settings in the program.

Fuel

The fuel composition is also set to be the default setting in the program. The composition will vary for different fuel type and therefore the default setting is used. LHV is set to be 41.4 MJ/kg. This is a typical LHV for heavy fuel. (Stapersma 2009) Since the settings for fuel quality are the same for all simulations and emission is not interesting for the output of the simulation, the accuracy is ok.

Crank arm ratio

Crank arm ratio is an input necessary to convert the results to depend on crank angle. The data required has not been available so a similar engine's data has been used to retrieve this input.

$$Cranck\ arm\ ratio = \frac{Crankshaft\ radius}{Conection\ rod\ length} \qquad (9.2)$$

Pressure difference between charge air and exhaust receiver pressure

This data is retrieved from the test bed results from appendix 13. The pressure difference here is 0.19 bars and is used for all simulations. The pressure difference for a real engine is likely to be reduced as the load and or the speed is reduced. Since such data are not available it has been assumed to be the same for the all simulations.

Pressure drop over intake and exhaust valves

This input represents the pressure drop over the valves. This data is not known so the pressure drop is kept zero for both intake and exhaust for all simulations.

Volume at start of compression

This parameter has been found using the same assumptions as for the compression ratio. The volume is the sum of the V_C and the V_{TDC}.

Compression and expansion

Both processes are assumed to be isentropic. The exponent kappa (κ) for the gas is calculated by the program based on the composition of gas in the cylinder.

Heat loss

The heat loss during combustion is set to be 10 %. The heat loss is not given from the engine data and is difficult to measure accurate. Measurements of cooling water temperature increase and flow can provide such results. In the simulation performed here it is set to 10 %, which is a normal range of heat loss for this kind of engine (Valland 2010).The heat loss to the cylinder walls will increase when the combustion temperature increase. This will not be taken into account in the simulations but will lead to a further increase in SFC.

Pressure difference for combustion at constant volume

The pressure difference is retrieved from the test bed results in appendix 13. The pressure difference at constant volume combustion is kept constant for all simulations. The max pressure is then determined by the compression pressure. The reduced max pressure is compensated by a longer combustion period during constant pressure, so that the target mean indicated pressure is kept constant for al simulations.

Air fuel ratio at end of combustion

This is initially set to 0.6. This parameter is set as a free variable so that the amount of fuel can be increased to reach the target mean indicated pressure.

Target mean indicated pressure

This parameter is kept constant for all simulations. The reason for this is to investigate how other parameters are affected by the reduced charge pressure for a fixed power output.

9.3.4. Simulation of 6L67GFCA

The simulation is performed according to the previous defined inputs. The results can be seen in the summary below and complete results are found in appendix 14-18. The mechanical efficiency is not stated in the data retrieved but was derived from the indicated and effective power output from the engine. This was found to be 0,93. The shaft power for these simulations is 6560 KW.

Charge air pressure	Bar	1,93	1,83	1,73	1,63	1,53
SFC indicated	g/kWh	170,8	172,2	172,90	174,30	175,70
SFC effective	g/kWh	183,66	185,16	185,91	187,42	188,92

Table 11 Results regarding SFC from the simulations
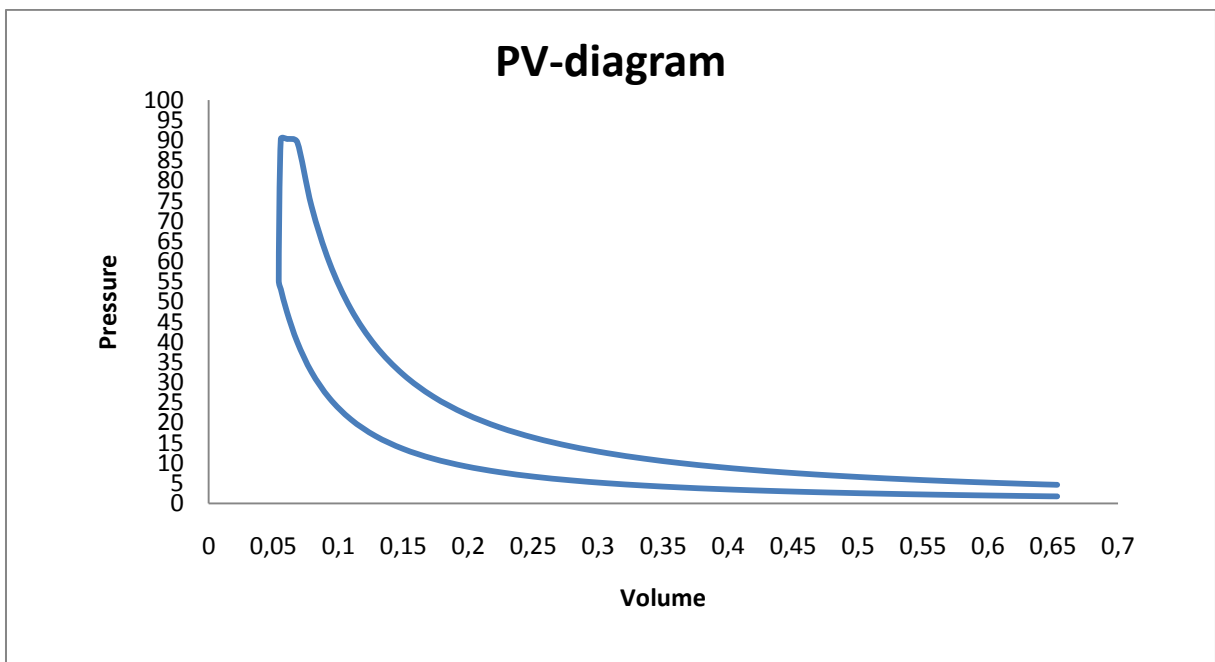
Figure 24 PV diagram from initial condition simulation with charge air pressure of 1,93 bar
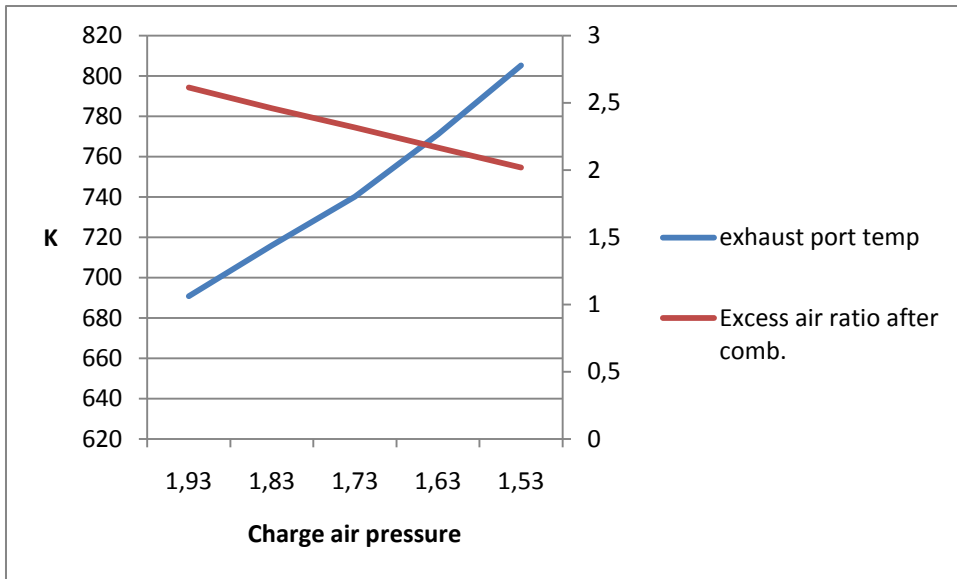
Figure 25 Simulated exhaust temperature and excess air ratio

As mentioned earlier there are several assumptions and simplifications done to perform these simulations. Since the same assumptions and simplifications are made for all simulations the results should indicate how a real engine process would react to the decreasing charge air pressure. The specific fuel consumption is increased by approximately 1g/kWh for each 0.1bar reduction in charge air pressure. This corresponds to the figures MAN B&W operate with when charge air pressure is reduced due to turbo charger malfunction (Bohni 2010).

9.3.5. Operation with reduced turbo charger performance

It has previously been shown how a simple performance analysis can give results on how the SFC will be increased due to reduced turbocharger efficiency. With a decrease of 0, 2 bars we can conservatively expect an increase of 2 g/kWh based on the simulation performed.

Caribbean
East and South Africa
East Coast South America
Far East
Gulf - Red Sea - India
Mediterranean
South East Asia
UK - Continent - Baltic
US Gulf
US West Coast
West Africa
West Coast South America

Table 12 Movement of the Siskin Arrow last 12 months(IHS-Fairplay 2010)

The MS Siskin Arrow is operating worldwide. A list of movements the last 12 months can be seen in table 12. A ship in this type of trade is normally operating at least 200 days a year, excluding time in harbour. According to Sea-web the Siskin Arrow has a rated power of 8249 KW.(IHS-Fairplay 2010) If the ship sails with 80% MCR it corresponds to a power of 6600KW. 0,2 bar reduction in charge air pressure will result in an extra fuel consumption of 63,360 ton for a year operation. Present IFO380 fuel oil price in Singapore is 435,5 US dollar per ton.(Bunkerworld 2010) The reduced charge air pressure will for this calculation example inflict an increased yearly bunker cost of approximately 27600US dollar a year.

This result is based on some assumptions regarding the sailing schedule for the ship that might deviate significantly from the actual sailing schedule, but provides a good pointer on how the decreased engine condition will lead to extra costs. The Siskin Arrow consumes 26 tonnes fuel per day according to Sea-Web so the engine condition results in almost three days of extra fuel consumption for the ship per year. It is unknown how much the charge air pressure is reduced, as new condition data for the ship in question is not available at the time.

The SFC might be the most interesting parameter to investigate since it is directly linked to the fuel consumption and cost. However, other elements should be taken into account when deciding if the turbo charger should be rebuilt or not. As can be seen in figure 25 the exhaust temperature will increase significantly when the TC condition is reduced. The temperature will reach max limits before the rated power is obtained. To avoid thermal overload, of especially exhaust valves and cylinder head, the power must be reduced and consequently also the ship's speed. This can also lead to reduced profit from the ship operation as the ships transport capacity will be reduced since each trip will require more time. Violating the temperature limits will over time lead to significantly increased maintenance costs. A way to gain the cruise speed for the vessel with the TC condition can be to reduce the cargo weight by loading less cargo or simply by choosing to transport lighter cargo. This will reduce the hull resistance and also the load of the engine. The consequence will most likely be reduced income.

The key to make the right decision must be based on the factors mentioned above. Accurate data must be used to do this right. In addition, the time required to repair and the cost of repairing must be known. This data and information gathering is outside the scope of this thesis, but the work done here provides a sound way of easy calculations that can be performed mainly regarding SFC and also how and which costs that should be included in such a decision.

9.4. Case conclusion; reduced turbine condition 2-stroke diesel engine

Performance analysis was in this chapter applied to a MAN B&W 2-stroke diesel engine. The reason for this was to determine the increase in SFC when TC condition was reduced. Such analysis can be helpful when decision regarding replacement or maintenance shall be taken.

The simulation of reduced turbine condition is responsible for approximately 1 g/kWh increase in fuel consumption for each 0,1 bar reduction in charge air pressure. The manufacturer operates with the same figures for this fault condition. Not all engine data were available when this analysis was performed. Assumptions have therefore been made regarding compression ratio and cylinder volume at TDC. The chapter regarding setup of the simulation is written so that it is easy to perform this simulation for other engine types.

The estimation for increase in costs based on increased fuel consumption is performed based on assumptions on the operation profile for the ship. With 200 in transit days a year increased costs amounts to 27600US dollar a year. The reduction in charge air pressure might result in reduced shaft power due to parameters exceeding limits. This effect has not been evaluated further.

10. Further work

The work done in this thesis is concentrated on some selected conditions. Further work on this topic will therefore be to expand the fault conditions to include more fault conditions for diesel engines. The computer program used can be set up to perform all kinds of experiments and analyses. This should be investigated thoroughly and can result in a more detailed analysis for certain areas. An example of this is the combustion model. When simulating the KRG-6 engine a relatively simple model was used. By implementing a predictive model the combustion process can be precisely modelled and more accurate results regarding NO_x and combustion development.

The K-type engine is an old engine and is no longer in production. A modern engine with higher efficiency and modern technology such as common rail or turbo chargers with variable inlet geometry would be interesting to apply performance analysis to, even if the basics of diesel engine principles are the same. The challenge would of course be to get the required data and model the engine accordingly in the simulation program.

The case study regarding MS Siskin Arrow would benefit from having more data available for the engine. Since this is an old vessel it has been difficult to get hands on a complete set of test bed data from new condition. Data for the ships operation pattern must be known if good estimations for the increased costs regarding fault conditions shall be possible to predict.

11. Literature and references

Bergen-Diesel (1993). Motor karrakteristikk Bergen-Diesel.

Bohni, J. (2010). "Interview."

Bunkerworld (2010). "Bunkerworld daily email."

Eilif Pedersen, H. V. (2008). Marint Maskineri.

G.Stiesch (2003). Modeling Engine Spray And Combustion Processes. Hannover, Springer.

GammaTechnologies (2006). User's manual.

Hatlevold, E. S. (2009). "Assessment of engine performance and exhaust emissions at changing operating conditions and under fault conditions."

Heywood, J. B. (1988). Internal combustion engine fundamentals McGraw-Hill, Inc.

Hountalas, D. T. (2000). "Prediction of marine diesel engine performance under fault conditions." Applied Thermal Engineering 20 (2000) 1753-1783.

IHS-Fairplay (2010). Sea web.

ISO-3046-1 (2002). " Reciprocating internal combustion engines-Performance."

Ken-ichi Kohashi, Y. F., Jin Kusaka and Yasuhiro Daisho (2003). "A numerical study on Ignition and combustion of a DI Diesel engine by using CFD Code combined with Detailed Chemical Kinetics." SAE International SP-1795 Modeling of Diesel &SI Engines.

MAN-B&W-Diesel-A/S "Ambient temperature operation and matching."

MAN-B&W-Diesel-A/S (1998). Instruction book OPERATION.

MAN-Diesel NR Turbochargers; economical.

N.E Chell, C., FIMarE (1999). Operation and Maintenance of Machinery in Motorships.

Rasmussen, M. (2003). Driftsteknikk grunnkurs.

Rolls-RoyceMarineAS (2001). Project guide for Marine Propulsion Plants, Bergen diesel type K. Rolls-Royce. Bergen.

Ryati, N. A. (2010). Personal communication.

Stapersma, D. (2009). Diesel engines A - Performance analysis.

Stapersma, D. (2009). Diesel engines; Combustion.

Stapersma, D. (2009). Diesel engines; Performance analysis.

Stapersma, D. (2009). Emissions and Heat transfer.

Stone, R. (1999). Introduction to Internal Combustion Engines.

Valland, H. (2008). "Computation of thermodynamic properties of combustion products and fuel-air processes."

Valland, H. (2010). Dialogue with Professor.

Valland(a), H. Power Cycle Process Diagrams.

Valland(c), H. (2008). Applications in Dynamic Process Analysis and Process Simulation. Trondheim, Marine Thechnology Centre.

12. List of appendix

Appendix 1 ISO correction of SFC for KRG-6 engine

Air temperature	Tra	298			
Total barometric pressure	pra	100			
Relative humidity	øra	30			
Charge air coolant temperature	Tcra	298			

Non reference condition

Air temperature	Tx	308	298	C
Total barometric pressure	px	100	100	kPa
Relative humidity	øx	30	30	%
Charge air coolant temperature	Tcx	298	298	C
Mech. Eff.		0,93	0,93	-

Coefficients from table 2

a	0	0	-
m	0,7	0,7	-
n	1,2	1,2	-
s	1	1	-

B.1	1,68	-
Dry air pressure ratio table B.2	0,99	-
k	0,9544	-
alfa	0,9520	-
beta calculated from equation 8; ISO 3046	1,0025	1,0000	-

SFC non reference	197,557	197,060	g/kWh
Difference	0,497	0,000	

Appendix 2 Bergen diesel KRG-6 engine characteristics

Engine characteristics					
Engine type	KRG-6				
Date	27.03.1993				
Speed	720	rpm	Torque	12532	Nm
Mean eff. pressure	17,82	bar			
Power	945	KW	Fuel mass	5,03	kg
Max cyl. pressure	136	bar	Fuel measuring time	96,6	sek
SFC	198,4	g/kWh			
Ambient pressure	1,022	bar	Pressure b. compressor	1,01	bar
Ambient temperature	22.feb	C	Pressure receiver	2,79	bar
Temp receiver	50,2	C	TC speed	31063	rpm
Air consumption	2,08	kg/s			
Temp. after cylinder 1	355	C	Exhaust mass flow	7665	kg/h
Temp. after cylinder 2	356	C			
Temp. after cylinder 3	357	C			
Temp. after cylinder 4	334	C			
Temp. after cylinder 5	334	C			
Temp. after cylinder 6	348	C			

Appendix 3 Comparison between simulation and test bed data

	Simulation	Test bed	
Mean effective pressure	17,8232	17,82	bar
SFC	197,517	198,40	g/KWh
Max pressure	129,615	136,00	bar
Max temperature	1711,48		K
Brake spec. NO_x	1,81461	1,70	g/KWh
Fuel air ratio	0,0310217		-
Exh temp after cylinder	641,951	628,00	K
Exh temp before turbine	693,863		K
Turbine			
TC speed	31283,2	31063,00	rpm
Average efficiency	77,9104		KW
Average power	272,4		KW
Compressor			
Average efficiency	76,6818		
Outlet pressure	2,84133		bar
Outlet temperature	428,469		K
Charge air cooler			
IC 2. stage outlet temp	315,889	323,20	K
IC 2. stage outlet pressure	2,8357	2,79	bar

Brake specific NO_x measurements are believed to be inaccurate for this engine running on diesel engine.

Appendix 4 Simulation results for increased ambient air temperature

| Engine load | KW | 945 |
| Engine speed | rpm | 720 |

Case		1	2	3	4	5
Ambient air temperature	K	275	285	295	305	315
Ambient sea temperature	K	298	298	298	298	298
Humidity	%	30	30	30	30	30
Ambient pressure	bar	1,022	1,022	1,022	1,022	1,022
Key performance parameters						
BSFC	g/KWh	195,799	196,655	197,517	198,402	199,323
Max pressure	bar	134,092	131,754	129,615	127,594	125,682
Max temperature	K	1658,62	1685,78	1711,48	1735,73	1757,06
Brake spec. Nox	g/KWh	1,71056	1,77384	1,81461	1,8195	1,76292
Brake spec. Nox	%	94,3	97,8	100,0	100,3	97,2
Fuel air ratio	-	0,028963	0,02999	0,031022	0,032071	0,033134
Exh temp after cylinder	K	620,229	631,179	641,952	652,8	663,426
Exh temp before turbine	K	670,366	682,231	693,862	705,44	716,603
Turbine						
TC speed	rpm	31181,9	31223,5	31283,2	31357,6	31455,9
Average efficiency	-	77,7843	77,8516	77,9104	77,9596	78,0026
Average power	KW	289,419	280,459	272,4	265,156	258,908
Compressor						
Average efficiency		76,4983	76,2939	76,0893	75,8831	75,6736
Outlet pressure	bar	2,9687	2,8854	2,8096	2,74011	2,67801
Outlet temperature	K	406,009	414,1	422,158	430,147	438,136
Charge air						
Temperature	K	315,14	315,19	315,221	315,225	315,209
Pressure	bar	2,96096	2,87797	2,80247	2,73326	2,67142

Appendix 5 Simulation results for increased ambient water temperature

Engine load	KW	945
Engine speed	rpm	720

Case		1	2	3	4
Ambient air temperature	K	298	298	298	298
Ambient sea temperature	K	273	283	293	303
Humidity	%	30	30	30	30
Ambient pressure	bar	1,022	1,022	1,022	1,022
Key performance parameters					
BSFC	g/KWh	195,51	196,282	197,033	197,782
Max pressure	bar	129,056	129,474	129,883	130,301
Max temperature	K	1664,23	1681,68	1698,68	1715,52
Brake spec. Nox	g/KWh	16,341	17,454	18,5888	19,7628
Brake spec. Nox	%	100	107	114	121
Fuel air ratio	-	0,0299544	0,0303145	0,0306629	0,031011
Exh temp after cylinder	K	624,748	630,123	635,357	640,64
Exh temp before turbine	K	675,872	681,356	686,69	692,048
Turbine					
TC speed	rpm	31201,6	31343,8	31489,5	31634,9
Average efficiency	-	79,2085	79,1906	79,1748	79,1599
Average power	KW	272,337	275,063	277,806	280,496
Compressor					
Average efficiency		76,1469	76,3753	76,5838	76,7741
Outlet pressure	bar	2,73726	2,77035	2,80384	2,83702
Outlet temperature	K	424,245	425,586	426,958	428,322
Charge air					
Temperature	K	296,402	304,067	311,735	319,399
Pressure	bar	2,73447	2,7675	2,80093	2,83405

Appendix 6 Simulation results for increasing ambient humidity

Engine load	KW	945
Engine speed	rpm	720

Case		1	2	3	4	5
Ambient air temperature	K	294,5	294,5	294,5	294,5	294,5
Ambient sea temperature	K	298	298	298	298	298
Humidity	%	30	40	50	60	70
Ambient pressure	bar	1,022	1,022	1,022	1,022	1,022
Key performance parameters						
BSFC	g/KWh	197,517	197,549	197,582	197,614	197,648
Max cyl. pressure	bar	129,615	129,591	129,56	129,533	129,504
Max cyl. temperature	K	1711,48	1710,26	1709,03	1707,8	1706,56
Brake spec. Nox	g/KWh	1,81461	1,77877	1,74292	1,71	1,67241
Brake spec. Nox	%	100	98,02492	96,049289	94,23512	92,163605
Fuel air ratio	-	0,031022	0,031039	0,0310553	0,031072	0,031089
Exh temp after cylinder	K	641,951	641,94	641,924	641,886	641,863
Exh temp before turbine		693,863	693,822	693,765	693,716	693,668
Turbine						
TC speed	rpm	31283,2	31291,6	31298,8	31306,5	31314,3
Average efficiency	-	77,9104	77,9092	77,9083	77,9073	77,9063
Average power	KW	272,4	272,709	272,978	273,268	273,557
Compressor						
Average efficiency	-	76,0893	76,087	76,0839	76,0812	76,0785
Outlet pressure	bar	2,8096	2,81096	2,81213	2,81339	2,81465
Outlet temperature	K	422,158	422,17	422,174	422,182	422,19
Charge air						
Temperature	K	315,221	315,217	315,211	315,206	315,201
Pressure	bar	2,80247	2,80384	2,805	2,80627	2,80753

Appendix 7 Simulation results for decreasing ambient pressure

Engine load	KW	945
Engine speed	rpm	720

Case		1	2	3	4	5
Ambient air temperature	K	294,5	294,5	294,5	294,5	294,5
Ambient sea temperature	K	298	298	298	298	298
Humidity	%	30	30	30	30	30
Ambient pressure	bar	1,022	0,972	0,922	0,872	0,822
Key performance parameters						
SFC	g/KWh	197,517	197,859	198,227	198,617	199,015
Max pressure	bar	129,615	128,649	127,679	126,697	125,737
Max temperature	K	1711,48	1723,86	1736,83	1750,26	1763,84
Brake spec. Nox	g/KWh	1,81461	1,85302	1,89406	1,93766	1,98207
Brake spec. Nox	%	100	102	104	107	109
Fuel air ratio	-	0,0310217	0,0314889	0,0319826	0,0324977	0,0330214
Exh temp after cylinder	K	690,7	695,649	701,116	706,732	712,601
Exh temp before turbine	K	693,863	698,831	704,149	709,75	715,444
Turbine						
TC speed	rpm	31283,2	31904,3	32590,9	33359,3	34232,8
Average efficiency	-	77,9104	77,767	77,6056	77,4494	77,3248
Average power	KW	272,4	280,528	289,006	298,002	307,796
Compressor						
Average efficiency		76,0893	76,0861	76,087	76,0954	76,1155
Outlet pressure	bar	2,8096	2,77455	2,73872	2,70258	2,66719
Outlet temperature	K	422,158	427,557	433,325	439,53	446,288
Charge air						
Temperature	K	315,221	315,351	315,479	315,614	315,767
Pressure	bar	2,80343	2,76848	2,73277	2,69673	2,66145

Appendix 8 Simulation results for reduced compressor efficiency

Case		1	2	3	4	5
Ambient air temperature	K	294,5	294,5	294,5	294,5	294,5
Ambient sea temperature	K	298	298	298	298	298
Humidity	%	30	30	30	30	30
Ambient pressure	bar	1,022	1,022	1,022	1,022	1,022
Compressor eff. reduction	%	100	95	90	85	80
Key performance parameters						
SFC	g/KWh	197,517	198,829	200,244	201,824	203,58
Max pressure	bar	129,615	126,166	122,847	119,56	116,332
Max temperature	K	1711,48	1755,93	1803,43	1856,13	1914,04
Brake spec. Nox	g/KWh	1,81461	1,96768	2,14652	2,36538	2,6296
Brake spec. Nox	%	100	108,435421	118,290983	130,351976	144,912681
Fuel air ratio	-	0,0310217	0,0327309	0,034586	0,0366798	0,039029
Exh temp after cylinder	K	641,951	660,059	680,17	703,323	729,728
Exh temp before turbine	K	693,863	713,847	735,614	760,257	788,034
Turbine						
TC speed	rpm	31283,2	30507,4	29721,9	28729,8	27628,2
Average efficiency	-	77,9104	77,7423	77,4999	77,0711	76,4483
Average power	KW	272,4	256,924	241,766	226,096	210,123
Compressor						
Average efficiency	-	76,0893	72,3701	68,6377	64,8433	61,0142
Outlet pressure	bar	2,8096	2,67724	2,54905	2,42058	2,29299
Outlet temperature	K	422,158	421,392	420,551	419,422	417,947
Charge air						
Temperature	K	315,221	314,32	313,425	312,507	311,563
Pressure	bar	2,80247	2,67052	2,54272	2,41464	2,28744

Appendix 9 Simulation results for reduced turbine efficiency

Engine load	KW	945
Engine speed	rpm	720

Case		1	2	3	4	5
Ambient air temperature	K	294,5	294,5	294,5	294,5	294,5
Ambient sea temperature	K	298	298	298	298	298
Humidity	%	30	30	30	30	30
Ambient pressure	bar	1,022	1,022	1,022	1,022	1,022
Turbine efficiency reduction	%	100	95	90	85	80
Key performance parameters						
BSFC	g/KWh	197,517	198,781	200,157	201,717	203,433
Max pressure	bar	129,615	126,17	122,84	119,532	116,328
Max temperature	K	1711,48	1754,72	1801,37	1853,73	1910,56
Brake spec. Nox	g/KWh	1,81461	1,96009	2,13241	2,34654	2,60219
Brake spec. Nox	%	100	108	118	129	143
Fuel air ratio	-	0,0310217	0,0326994	0,034533	0,0366201	0,0389313
Exh temp after cylinder	K	641,951	659,611	679,453	702,552	728,562
Exh temp before turbine	K	693,863	713,379	734,862	759,457	786,822
Turbine						
TC speed	rpm	31283,3	30505,9	29715,9	28713,1	27616,1
Average efficiency	-	77,9104	73,8567	69,753	65,5122	61,171
Average power	KW	272,4	244,064	217,518	192,009	168,013
Compressor						
Average efficiency	-	76,0893	76,17	76,2461	76,2591	76,2393
Outlet pressure	bar	2,8096	2,67674	2,54772	2,41805	2,2911
Outlet temperature	K	422,158	415,141	408,103	400,869	393,554
Charge air						
Temperature	K	315,221	313,95	312,739	311,563	310,437
Pressure	bar	2,80247	2,66998	2,54133	2,41201	2,28543

Appendix 10 Simulation results for variation in injection timing (advanced timing)

Engine load	KW	945
Engine speed	rpm	720

		Later injection				Original. Setting
Case		1	2	3	4	5
Ambient air temperature	K	294,5	294,5	294,5	294,5	294,5
Ambient sea temperature	K	298	298	298	298	298
Humidity	%	30	30	30	30	30
Ambient pressure	bar	1,022	1,022	1,022	1,022	1,022
Injection start rel. To TDC	deg	-8,50	-9,50	-10,50	-11,50	-12,50
Key performance parameters						
BSFC	g/KWh	201,128	200,075	199,117	198,263	197,517
Max pressure	bar	117,336	120,285	123,336	126,437	129,615
Max temperature	K	1660,7	1673,05	1685,45	1698,25	1711,48
Brake spec. Nox	g/KWh	1,46299	1,54395	1,62914	1,71963	1,81461
Brake spec. Nox	%	81	85	90	95	100
Fuel air ratio	-	0,0303615	0,0305355	0,0306967	0,030859	0,0310217
Exh temp after cylinder	K	647,765	646,306	644,76	643,309	641,951
Exh temp before turbine	K	700,613	698,92	697,127	695,447	693,863
Turbine						
TC speed	rpm	31977,2	31782,8	31605,2	31438,5	31283,2
Average efficiency	-	77,7441	77,7889	77,8325	77,873	77,9104
Average power	KW	297,435	290,429	283,989	277,983	272,4
Compressor						
Average efficiency		76,1074	76,1002	76,0958	76,0921	76,0893
Outlet pressure	bar	2,93072	2,89678	2,86583	2,83675	2,84133
Outlet temperature	K	428,201	426,531	424,99	423,531	428,469
Charge air						
Temperature	K	316,319	316,01	315,729	315,466	315,889
Pressure	bar	2,92432	2,89045	2,85955	2,83053	2,80343

Appendix 11 Simulation results for variation in injection timing (retarded timing)

Engine load	KW	945
Engine speed	rpm	720

Case		6	7	8	9
Injection start rel. To TDC	deg	-13,50	-13,50	-14,50	-15,50
Key performance parameters					
BSFC	g/KWh	196,885	196,347	195,918	195,599
Max cyl pressure	bar	132,833	136,114	139,476	142,895
max cyl temperature	K	1725,5	1739,53	1753,96	1768,75
Brake spec. NO_x	g/KWh	1,9167	2,02259	2,13434	2,25104
Brake spec. NO_x	%	106	111	118	124
Fuel air ratio	-	0,0311964	0,0313582	0,031519	0,0316782
Exh temp after cylinder	K	640,842	639,65	638,572	637,564
Exh temp before turbine	K	692,559	691,18	689,907	688,742
Turbine					
TC speed	rpm	31134,5	31001,3	30879,6	30769,2
Average efficiency	-	77,9432	77,9742	78,0022	78,0276
Average power	KW	267,156	262,422	258,108	254,214
Compressor					
Average efficiency		76,0852	76,0834	76,082	76,0811
Outlet pressure	bar	2,81477	2,79103	2,76933	2,74963
Outlet temperature	K	427,128	425,919	424,805	423,788
Charge air					
Temperature	K	315,648	315,431	315,234	315,055
Pressure	bar	2,77745	2,75424	2,733	2,71375

Appendix 12 Simulation results for reduced charge air cooler efficiency

Engine load	KW	945
Engine speed	rpm	720

Case		1	2	3	4	5
Ambient air temperature	K	294,5	294,5	294,5	294,5	294,5
Ambient sea temperature	K	298	298	298	298	298
Humidity	%	30	30	30	30	30
Ambient pressure	bar	1,022	1,022	1,022	1,022	1,022
Cooler efficiency reduction	%	100	90	80	70	60
Key performance parameters						
BSFC	g/KWh	197,517	198,093	198,666	199,237	199,81
Max pressure	bar	129,615	129,966	130,324	130,664	131,02
Max temperature	K	1711,48	1724,81	1737,86	1750,93	1764,06
Brake spec. Nox	g/KWh	1,81461	1,9058	1,99928	2,09506	2,19492
Brake spec. Nox	%	100	105	110	115	121
Fuel air ratio	-	0,031021	0,031288	0,031546	0,0318	0,032071
Exh temp after cylinder	K	641,951	646,175	650,36	654,638	658,942
Exh temp before turbine	K	693,863	698,152	702,352	706,604	710,896
Turbine						
TC speed	rpm	31283,2	31397,5	31517,7	31638,6	31759,9
Average efficiency	-	77,9104	77,8973	77,8854	77,8736	77,8617
Average power	KW	272,4	274,643	276,977	279,288	281,601
Compressor						
Average efficiency	-	76,0893	76,2746	76,4454	76,6039	76,7513
Outlet pressure	bar	2,8096	2,83669	2,86462	2,89249	2,92042
Outlet temperature	K	422,158	423,214	424,322	425,433	426,551
Charge air						
Temperature	K	315,221	321,332	327,5	333,721	339,995
Pressure	bar	2,80247	2,82947	2,8573	2,88507	2,9129

Appendix 13 Test bed data for MAN B&W 6L67 GFCA engine

Test bed data for 100,5 % load and 123 rpm are presented on the next page, this is not the same engine as MS Siskin Arrow has but a developed engine with higher speed and power limit. In addition original test bed date for 107 and 117rpm are presented on the CD attached to the report. This file was to large to be posted in its hole content here.

TESTBED DATA	Engine Type:	L67GFCA	Water Brake:	FROUDE	No.:		Constant, K:	0,07	kW/Kg.RPM	MAN
	Engine Builder:	GOETAV	Engine No.:		Yard: Fincantieri Genova Sestri Yard					

Layout kW:	9635,05	Layout RPM:	123	Sign.:				Test No.:	1

Turbocharger(s)		No. of TC:	1		Serial No.	No. of Cyl.:	6	Bore, m:	0,67	Stroke, m:	1,700
Make:	ABB	Type:	VTR631-1-G	1		Cylinder Constant (kW,bar):	0,9989	Mean Friction. Press., bar:	1,00		
Max. RPM:		Max. Temp., °C:		2		Lubrication Oil System (Tick box)					
Compr. Slip Factor:	0,890	Compr. Diam., m:	0,7608	3		[X] Internal	[ ] External from M. E. System		[ ] External from Gravity Tank		
TC specification:		GB7T52.3IVCG605W14Z4		4							

Observation No: 11

Fuel Oil Viscosity:		at:	50	°C			Brand		Type	
Bunker Station:					Cylinder Oil					
Oil Brand:		Heat value, kcal/kg:			Circulating Oil					
Density at 15 °C:		Sulphur, %:			Turbo Oil					

Test Date (yyyy-mm-dd)	Test Hour (hh:mm)	Load %	Ambient Pressure mbar	Water Brake Load Kg	Engine RPM	Governor index	Speed Setting bar	VIT Control bar
1983-05-18		100,5	1008	1064,0	123,7			

Effective Power kW	Indicated Power kW	Eff. Fuel Consumption g/kWh	Indicated Fuel Consumption g/kWh
9681		192,11	

Cylinder No.	1	2	3	4	5	6	7	8	9	10	11	12	13	14	15	16	17	18	Ave.
Pi, bar																			
Pmax, bar	97,0	96,5	95,0	94,5	95,0	95,5													95,6
Ref. Pmax, bar																			
Pcomp, bar	79,5	81,0	81,0	81,0	81,5	81,0													80,8
Fuel Pump Index	104,0	104,0	105,0	108,0	102,0	105,0													104,7
VIT index																			
Exhaust Gas Temp., °C	375	350	335	355	370	365													358,3
Cooling Water Outlet Temp., °C																			
Piston Outlet Lub. Temp., °C																			

Cooling Water Temperature, °C				Exhaust Gas Temp., °C			Exhaust Pressure		Turbo Charger	Aux. Blower	Scavenge Air Pressure		
Air Cooler		Main Engine		Turbine			Receiver	Turb. Outl.			▲p Filter	▲p Cooler	Receiver
Inlet	Outlet	Inlet	Turb. Outlet	Inlet	Outlet		bar	mmWC	RPM	On/Off	mmWc	mmWc	bar
1	1	70	1	1	1		1,74	1	1	Off	1	1	1,93
29	40	Seaw. Temp.	77,0	415	278		mmHg	0	9930	Axial Vibration	15	130	mmHg
2	2		2	2	2		1305	2	2		2	2	1450
										mm			
3	3		3	3	3			3	3		3	3	
4	4		4	4	4			4	4		4	4	
Ave.	Ave.		Ave.	Ave.	Ave.			Ave.	Ave.		Ave.	Ave.	
29	40		77	415	278			0	9930		15	130	

Scavenge Air Temperature, °C				Lubricating Oil				Fuel Oil Pressure
	Inlet Blower	Before Cooler	After Cooler	Pressure, bar	Temperature, °C	Temperature, °C		bar
Scavenge Air Temperature	1	1	1	System Oil	Inlet Engine	TC Inlet / Blower end	TC Outlet / Turb. end	Before Filter
	23,0	162	41	2,15	45,0	1	1	After Filter
41	2	2	2	Cooling Oil	Inlet Cam			
				2,20	36,0			8,0
	3	3	3	Cam Shaft Oil	Outlet Cam	2	2	Temperature, °C
				3,05				Before Pumps
	4	4	4	Turbine Oil	Thrust Segment	3	3	
	Ave.	Ave.	Ave.					
	23,0	162	41			4	4	
						Ave.	Ave.	

Remarks: SHOPTRIAL NO1. LCV ESTIMATED.EXHAUST CAM +1DEGR. PISTON LIFTET 8MM. VIT-FUEL PUMPS.

Appendix 14 Simulation results for B&W 6L67GFCA; charge air pressure 1.93 bar

(Red numbers are outputs from simulation, black numbers are calculated based on the outputs)

```
                                     Work       MIP
                                     [kJ]       [bar]
Gross                              659,323          11
Pumping                             11,088      0,185
Net                               670,411     11,185

Power Cycle Performance Summary:
Inlet port pressure                    1,93 [bar]
Inlet temperature                       314 [K]
Compression pressure                   55,3 [bar]
Max cylinder pressure                  90,3 [bar]
Mean indicated pressure                  11 [bar]
Mean pumping pressure                 0,185 [bar]
Indicated specific fuel consumption  0,1708 [kg/kWh]
Indicated specific air consumption     6,59 [kg/kWh]
Excess air ratio after combustion     2,612 [-]
Exhaust port pressure                  1,74 [bar]
Exhaust port temperature              690,7 [K]
```

Mechanical efficiency	0,93	
Comparison speed	107,00	Rpm
Indicated power (cylinder)	1195,57	KW
Effective power (cylinder)	1111,88	KW
Shaft power	6671,26	KW
SFC indicated	170,80	g/kWh
SFC effective	**183,66**	g/kWh

Appendix 15 Simulation results for B&W 6L67GFCA; charge air pressure 1.83 bar

(Red numbers are outputs from simulation, black numbers are calculated based on the outputs)

```
                                     Work      MIP
                                     [kJ]      [bar]
Gross                                659,305        11
Pumping                               11,034    0,184
Net                                  670,339   11,184

Power Cycle Performance Summary:
Inlet port pressure                    1,83 [bar]
Inlet temperature                    314,00 [K]
Compression pressure                  52,45 [bar]
Max cylinder pressure                 87,45 [bar]
Mean indicated pressure               11,00 [bar]
Mean pumping pressure                  0,18 [bar]
Indicated specific fuel consumption    0,17 [kg/kWh]
Indicated specific air consumption 45809,00 [kg/kWh]
Excess air ratio after combustion      2,46 [-]
Exhaust port pressure                  1,64 [bar]
Exhaust port temperature             716,04 [K]
```

Mechanical efficiency	0,93	
Comparison speed	117,00	Rpm
Indicated power (cylinder)	1285,64	KW
Effective power (cylinder)	1195,65	KW
Shaft power	7173,90	KW
SFC indicated	172,20	g/kWh
SFC effective	185,16	g/kWh

Appendix 16 Simulation results for B&W 6L67GFCA; charge air pressure 1.73 bar

(Red numbers are outputs from simulation, black numbers are calculated based on the outputs)

	Work [kJ]	MIP [bar]
Gross	659,3	11
Pumping	10,988	0,183
Net	670,288	11,183

```
Power Cycle Performance Summary:
Inlet port pressure                        1,73 [bar]
Inlet temperature                           314 [K]
Compression pressure                      49,61 [bar]
Max cylinder pressure                     84,61 [bar]
Mean indicated pressure                      11 [bar]
Mean pumping pressure                     0,183 [bar]
Indicated specific fuel consumption      0,1729 [kg/kWh]
Indicated specific air consumption         5,92 [kg/kWh]
Excess air ratio after combustion         2,316 [-]
Exhaust port pressure                      1,54 [bar]
Exhaust port temperature                   740,1 [K]
```

Mechanical efficiency	0,93	
Comparison speed	107,00	Rpm
Indicated power (cylinder)	1175,75	KW
Effective power (cylinder)	1093,45	KW
Shaft power	6560,69	KW
SFC indicated	172,90	g/kWh
SFC effective	185,91	g/kWh

Appendix 17 Simulation results for B&W 6L67GFCA; charge air pressure 1.63 bar

(Red numbers are outputs from simulation, black numbers are calculated based on the outputs)

	Work [kJ]	MIP [bar]
Gross	659,31	11
Pumping	10,935	0,182
Net	670,245	11,183

```
Power Cycle Performance Summary:
Inlet port pressure                      1,63 [bar]
Inlet temperature                         314 [K]
Compression pressure                    46,76 [bar]
Max cylinder pressure                   81,76 [bar]
Mean indicated pressure                    11 [bar]
Mean pumping pressure                   0,182 [bar]
Indicated specific fuel consumption    0,1743 [kg/kWh]
Indicated specific air consumption       5,58 [kg/kWh]
Excess air ratio after combustion       2,165 [-]
Exhaust port pressure                    1,44 [bar]
Exhaust port temperature               771,09 [K]
```

Mechanical efficiency	0,93	
Comparison speed	107,00	rpm
Indicated power (cylinder)	1175,77	KW
Effective power (cylinder)	1093,47	KW
Shaft power	6560,79	KW
SFC indicated	174,30	g/kWh
SFC effective	187,42	g/kWh

Appendix 18 Simulation results for B&W 6L67GFCA; charge air pressure 1.53 bar

(Red numbers are outputs from simulation, black numbers are calculated based on the outputs)

```
                                      Work      MIP
                                      [kJ]      [bar]
Gross                                 659,31        11
Pumping                               10,879    0,182
Net                                   670,189   11,182

Power Cycle Performance Summary:
Inlet port pressure                     1,53 [bar]
Inlet temperature                        314 [K]
Compression pressure                   43,92 [bar]
Max cylinder pressure                  78,92 [bar]
Mean indicated pressure                   11 [bar]
Mean pumping pressure                  0,182 [bar]
Indicated specific fuel consumption   0,1757 [kg/kWh]
Indicated specific air consumption      5,24 [kg/kWh]
Excess air ratio after combustion      2,018 [-]
Exhaust port pressure                   1,34 [bar]
Exhaust port temperature              805,14 [K]
```

Mechanical efficiency	0,93	
Comparison speed	107,00	Rpm
Indicated power (cylinder)	1175,77	KW
Effective power (cylinder)	1093,47	KW
Shaft power	6560,79	KW
SFC indicated	175,70	g/kWh
SFC effective	188,92	g/kWh

Appendix 19 Comparison calculations ambient condition

		1165			
Engine load	KW	(100%)			
Engine speed	rpm	720			

Ambient air temp	K	273	283	298	308
Ambient sea temp	K	298	298	298	298
Ambient humidity	%	30	30	30	30
Ambient pressure	kPa	100	100	100	100

Key performance parameters

SFC	g/KWh	194,77	195,654	197,06	198,263
Max pressure	bar	155,948	153,209	149,19	146,555
max temperature	K	1679,91	1708,61	1751,63	1768,64
Brake spec. Nox	g/KWh	1,81976	1,89244	1,9663	1,7088

Non reference condition

Air temperature	Tx	278	288	298	308	C
Total barometric pressure	px	100	100	100	100	kPa
Relative humidity	øx	30	30	30	30	%
Charge air coolant temperature	Tcx	298	298	298	298	C

Mech. Eff.		0,93	0,93	0,93	0,93	-

Coefficients from table 2

a		0	0	0	0	-
m		0,7	0,7	0,7	0,7	-
n		1,2	1,2	1,2	1,2	-
s		1	1	1	1	-

B.1		0,25	0,5		1,68	-
Dry air pressure ratio table B.2		1,0075	1,005		0,99	-
k		1,0926	1,0455		0,9544	-
alfa		1,0975	1,0478		0,9520	-
beta calculated from equation 8; ISO 3046		0,9956	0,9977	1,0000	1,0025	-

SFC non reference (Iso-corr)	196,184	196,610	197,060	197,557	g/kWh
Difference	-0,876	-0,450	0,000	0,497	

Results from simulation	194,77	195,654	197,06	198,018	g/kWh
Difference	-2,29	-1,406	0	0,958	

MOTORKARAKTERISTIKK BERGEN DIESEL
PROSJEKT NR.   MOTOR 3499 KRG-6
MOTORTYPE   DYSERING EF16

EF-16 27.03.93
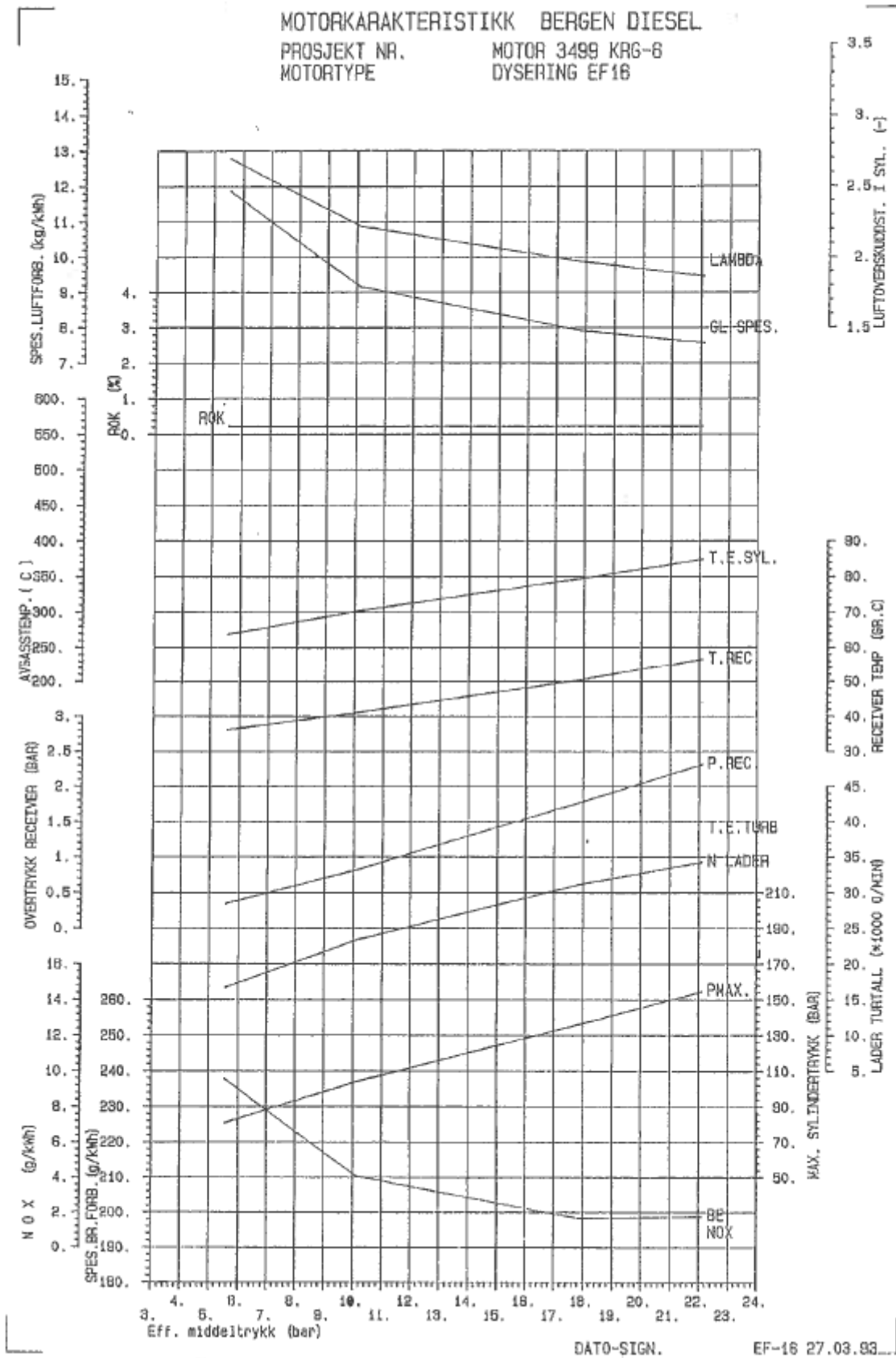
```
*******************************************************************
*                   MOTORKARAKTERISTIKK BERGEN DIESEL             *
*                   PROSJEKT  :MOTOR 3499 KRG-6                    *
*                   MOTORTYPE :DYSERING EF16                       *
*******************************************************************
FORSØK NR.   9    UTFØRT DATO: 27. 3.93.      KLOKKESLETT:  14.35.54.
*******************************************************************


MOTOR-TURTALL      (o/min)  720.0  DREIEMOMENT          (Nm) 12532.
EFF.MIDDELTRYKK      (bar)   17.82 BREMSEKRAFT            (N)     0.
YTELSE              (kW)    944.9  BRENNOLJEMENGDE       (kg)    5.030
MAKS.SYLINDERTRYKK  (bar)   136.0  BRENNOLJEMÅLING      (sek)   96.6
SPES.BRENNST.FORB.(g/kWh)   198.4  PÅDRAG               (mm)    24.5
                                   BRENNOLJETEMP. F.MOTOR (C)    0.0
*******************************************************************


BAROMETER    (bar)    1.022    TRYKKFALL LM.DYSE (mbar)    21.09
TETTHET    (kg/m3)    1.205    TRYKKTAP  LM.DYSE (mbar)    12.65
TEMP.F.LM.DYSE(C)    22.2      TRYKK F.LADER(abs) (bar)     1.01
TEMP.F.LADER   (C)   22.2      TRYKK REC.   (abs) (bar)     2.79
TEMP.E.LADER   (C)    0.0      OVERTRYKK REC.     (bar)     1.77
TEMP.RECEIVER (C)    50.5


KOEFF.LM.DYSE  (-)    .129     LADERTURTALL     (o/min) 31063.
LUFTMENGDE (kg/s)    2.08      LADERT.(298K)    (o/min) 31210.
LUFTVOLUM   (m3/s)   1.72      ADIAB.TEMP.STIGN.    (C)    97.4
LUFTV.298K (m3/s)    1.75      TRYKKFORHOLD O.LADER (-)     2.76
SP.LUFTF.(kg/kWh)    7.91      ADIAB.VIRKNINGSGRAD  (-)    -4.39
LAMBDA SYL.   (-)    1.97      LAMBDA AVGASS        (-)     2.81
SPYLEFAKTOR   (-)    1.43

AVGASSMÅLING                   AVGASSMÅLING KORR.(15 % O2)

NOX        (ppm)     0.0       NOX           (ppm)     0.0
NOX      (g/kWh)     0.0       NOX          (mg/m3)    0.0
THC        (ppm)     0.0       THC           (ppm)     0.0
O2         ( % )     0.0       CO2           ( % )     0.0
CO2        ( % )     0.0       CO            (ppm)     0.0
CO         (ppm)     0.0       CO           (mg/m3)    0.0


TEMP.E.SYL.1  (C) 355.      TEMP.  F.TURB. R1   (C)    0.
           2   "  356.        "        "     R2   "    0.
           3   "  357.        "        "     R3   "    0.
           4   "  334.      MIDDEL F.TURB.      "    0.
           5   "  334.      TEMP.  E.TURBIN     "    0.
           6   "  348.      AVGASSMENGDE     (kg/h) 7655.
           7   "    0.      RØKMÅLING  (1*BOSCH) (%)   .23
           8   "    0.
           9   "    0.
MIDDEL E.SYL.  "  347.
*******************************************************************

KJØLEVANN-SMØREOLJEDATA

KJØLEVANN-TEMP. F.MOTOR   75.8   E.MOTOR   79.9   TRYKK E.MOTOR  3.8
SMØREOLJE-TRYKK F.FILTER   4.9   E.FILTER   4.9
SMØREOLJE-TEMP. F.MOTOR   55.5   E.MOTOR   66.2
```